sTs®
Ann Arbor, Michigan

STS INCORPORATED
SCIENTIFIC TRANSLATION SERVICE
formerly Technical Library Research Service

OXIDE-CERMET FUEL RODS: PRODUCTION, PROPERTIES AND IRRADIATION BEHAVIOR

By P. Weimar and H. Zimmermann

KFK-1839, Aug 1973, 55 pp.

Translated from the German
For Argonne National Laboratory
P. O. No. 773790
Letter Release No. 11

STS Order No. 15397

ANL-TRANS-958

ARGONNE NATIONAL LABORATORY
Argonne, Illinois

OXIDE-CERMET FUEL RODS: PRODUCTION, PROPERTIES AND IRRADIATION BEHAVIOR

(Oxid-Cermet-Brennstäbe: Herstellung, Eigenschaften und Bestrahlungsverhalten)

by
P. Weimer, N. H. Zimmerman

Source: Kernforschungszentrum Karlsruhe
Institut für Material-und Festkörperforschung
KFK-1839 August 1973 51 pp.

Translated from German
by
STS Incorporated
July 1974

STS
Ann Arbor, Michigan

STS INCORPORATED
SCIENTIFIC TRANSLATION SERVICE
formerly Technical Library Research Service

OXIDE-CERMET FUEL RODS: PRODUCTION, PROPERTIES AND IRRADIATION BEHAVIOR

By P. Weimar and H. Zimmermann
Nuclear Research Center, Karlsruhe
Institute of Materials and Solid State Research
KFK 1839, August 1973

Gesellschaft für Kernforschung MBH, Karlsruhe

This report is based on studies concerning the fabrication of cermet fuel rods and determinations of their properties at the IMF and on the results of post-irradiation studies in the hot cells and at IRCh; we are indebted to all staff members of IMF, IRCh and RBT for making these facilities available to us and working with us, particularly Dr. Schneider (Mrs.) and F. Bauer, J. Burbach (IMF), Dr. Wertenbach (IRCh), P. Brunner, H. Enderlein, B. Schweigel (RBT/Z), R. Pejsa and especially Mr. F. Weiser (RBT/CuM), who very carefully conducted the extensive metallographic studies in good collaboration with IMF and thus contributed considerably toward the completion of this report.

Abstract

Oxide cermet fuel pins with idealized fuel structure and metallurgically bonded cladding have some properties which cannot be obtained by pins with oxide pellets. The continuous metal network in the fuel provides a considerably larger thermal conductivity and a lower central temperature during irradiation. The lower central temperature and the metallic envelopment of the fissionable oxide particles decrease or prevent the release of fission gases and volatile fission products. Therefore, the absence of a gas plenum is characteristic of cermet pins. For use in fast reactors only Cr and V are potential matrix metals because of their low cross sections for fast neutrons.

The cermets with idealized structure were produced by metallizing UO_2 spheres with Cr, V, or Mo by a vapor-deposition process. The spheres are vibrated into the cladding tubes, for instance in Inconel 625 or Hastelloy X tubes in the case of UO_2-Cr cermets. After electron beam welding of the tubes the pins are isostatically hot-pressed in He atmosphere. The metal content of the cermets was 20 and 30%, respectively. Some properties of the UO_2-Cr, UO_2-V, and UO_2-Mo cermets are described.

Seven irradiation capsules, one with UO_2-Mo, four with UO_2-Cr, and two with UO_2-V samples, were irradiated in the FR 2 reactor at mean rod powers of 470 - 700 W/cm and mean cladding temperatures of about 600°C to 10 - 95 MWd/kg U burnup. Each of the capsules contained eight or four fuel rod samples.

UO_2-30 vol.-% Cr cermets with Inconel 625 cladding were irradiated to 60 and 95 MWd/kg U burnup without showing any failure. At these burnups the Hastelloy X claddings were probably damaged by microcracks. However, the temperatures of the Hastelloy X claddings were nearly 100°C higher than those of the Inconel 625 claddings. The high burnup UO_2-Cr samples with Inconel 625 or Hastelloy X cladding did not show dimensional changes in any case. The samples with 20% Cr showed a depletion of Cr in the fuel centre region. Cr had been evaporated and condensed in the outer regions of the fuel. No such depletion was found in the cermet fuel with 30% Cr. The vanadium claddings of the UO_2-V cermets were damaged by many cracks in consequence of oxygen embrittlement during irradiation.

Bearing in mind that the disintegration of the idealized cermet structure limits the central temperature it is suggested that UO_2-30% Cr fuel pins can be operated with linear rod powers of about 800 W/cm and cladding temperatures of 650°C to burnups of 60 MWd/kg U and probably more. A further increase of the rod power can be achieved only with a matrix metal heaving a lower vapor pressure.

Table of Contents

1. Introduction

The concept of an oxide-cermet fuel rod with a metallurgical bonded cladding is promising to have a few properties which can not be realized with a pure oxide pellet fuel. The continuous metal network present in the cermet gives the fuel a significantly improved thermal conductivity and thus a lower core temperature during service in the reactor. The metal bond between fuel and cladding acts in the same direction. This results in a higher permissible rod power and lower fission gas release. The latter effect should be further enhanced by the metal coatings of the fuel particles. Consequently, the fission gas plenum in cermet fuel rods can be omitted. However, useful results with cermet fuel pins may be expected only if they have a certain fuel porosity because this will relieve the cladding from the mechanical stress produced by swelling of the fuel. By including a metal matrix and hot-press bonding between fuel and cladding, a notable strength increase of the fuel pin is obtained.

At the Karlsruhe Nuclear Research Center, oxide-cermet fuel pins were considered for two different types of reactors:

For a gas-cooled fast breeder [1]: However, in the first design of such a reactor, only a conservative fuel element with oxide pellets, a stainless steel cladding and fission gas plenum can be considered. A more advanced concept is offered by the higher cooling gas temperatures with so-called coated particle fuel. The cermet concept (oxide-Cr or V) therefore was not taken into account.

For a fast high-flux test reactor [2], we investigated an oxide-stainless steel variant. Isostatic hot pressing and extrusion were investigated as fabrication methods [3]. The objective of this reactor project closed the chapter on these cermets, since they are not suitable for fast power reactors because of their relatively high metal content and the absence of fertile material.

When the oxide-cermet fuels were abandoned for the above reasons, they aroused some interest in a few Russian studies [4]. In 1972, Nesterenkow et al. introduced a concept for a gas-cooled reactor in which the cermet fuel pins discussed here were considered as possible fuel elements. However, thus far, this N_2O_4-cooled reactor has received attention only by a general study and by investigations of cooling circuits and the radiation stability of the N_2O_4 coolant.

2. Fabrication

To fabricate a cermet fuel having the most favorable properties with a so-called idealized structure, a fuel phase with spherical particles is necessary as the starting material. Spherical UO_2-particles were employed as the starting material for the experiments described here. In part they were fabricated by a modified sol-gel process with subsequent sintering (Nukem, Federal Republic of Germany), and in part by an agglomeration process (Risley, England). The UO_2-particles had a diameter of about 110 µm. This starting material was subsequently metallized by a vapor deposition process. Coating was based on pentachloride in the case of molybdenum, tetrachloride for vanadium and an organic chromium compound for chromium [5,6,7]. These three metals are deposited at different rates and different purities from the gas phase by thermal decomposition of these compounds. A coating thickness of about 6 µm on 100 µm spheres results in a metal content of about 30 vol.% for the cermets. The metallized UO_2 spheres were subsequently loaded into the metallic cladding by vibratory compaction, the claddings were then sealed by electron beam welding and subjected to isostatic hot-bonding [8]. The autoclave used for hot-bonding is shown in Fig. 1, while Fig. 2 shows the pressure-temperature cycle in isostatic hot-bonding. The relation between bonding pressure and integral cermet density at T = const is shown in Fig. 3.

3. Mechanical and Physical Properties of the Cermet Fuel

To characterize the mechanical properties, bending tests (4-point support) were performed at a loading rate of 1 mm/min [9]. The dependence of the bending strength on the metal concentration observed for UO_2/Mo-, UO_2/Cr- and UO_2/V-cermets is shown in Fig. 4. It can be seen that the first two types of cermets exhibit a sharp minimum on the low-metal side with about 6 and 12 vol.% metal. For UO_2/V, this minimum probably falls between 15 and 20 vol.% metal. The position of these minima appears to be related with the different integrity of the metal component in the cermet. The presence of numerous stress concentrations by discontinuities within the coatings with a low metal content leads to a strength loss of the cermet to values lower than those of pure ceramics. Evidently the position of the minimum is largely determined by the high-temperature plasticity of the metal component, i.e. its behavior during the hot-bonding process.

With a similar high-temperature plasticity of ceramics and metal, an optimum structure appears to be obtained as a result of a low-defect metal coating. With higher metal concentrations, a marked strength increase occurs with UO_2/Mo and UO_2/Cr, and the values obtained are fairly high. However, for cermets with a vanadium matrix only a relatively minor improvement in bending strength was observed with increasing V concentration [10]. Furthermore, the dependence of the bending strength on the test temperature in a high vacuum was also determined. Fig. 5 shows the data for UO_2/Mo cermets and Fig. 6 for UO_2/30 vol.% Cr and UO_2/45 vol.% V cermets in a comparison. With the exception of UO_2/30 vol.% Mo, a decrease in bending strength of about 30% can be observed at 1000°C compared to room temperature. The UO_2/30 vol.% Cr cermet exhibits the same temperature dependence as UO_2/45 vol.% V (Fig. 6). The results obtained thus far indicate that the bond between cermet and cladding obtained by isostatic hot-pressing leads to higher fatigue strength values in the UO_2/Cr cermets with a heat-resistant cladding material. A 3-point bending-creep test device served to record creep curves in a high vacuum at 900°C for uncladded as well as cladded cermets. The endurance as a function of the bending stress is shown in Fig. 7. The difference between bare and cladded UO_2/30 vol.% Cr cermets is striking. The corresponding curve for UO_2/V cermets with a pure vanadium cladding has been plotted for a comparison.

Conductivity measurements were made with the UO_2/Mo-, UO_2/Cr- and UO_2/V-cermets. Measurements were made of the electrical conductivity [11] as a concentration and temperature function as well as the concentration-dependent thermal conductivity [8]. Fig. 8 shows the dependence of the specific electrical resistance on the metal concentration for three and five different metal concentrations. A marked decrease of the electrical resistance with increasing metal content can be observed; compared to pure UO_2, the electrical conductivity in UO_2/30 vol.% Mo-cermet shows an increase by about 11-12 orders of magnitude. Figs. 9 and 10 represent the temperature functions of the specific electrical resistance ρ for UO_2/Mo and UO_2/Cr cermets. The ρ-function is parallel to that of the matrix metal even up to temperatures of 1000°C, i.e. the UO_2 present in high concentration does not have a significant influence on conductivity [4]. Fig. 11 shows the resistance values for UO_2/30 vol.% metal cermets as a

function of temperature; a rise with increasing temperature is apparent; the resistance values increase from the Mo-containing to the Cr- and then to the V-containing cermets as is suggested by the data of the base metals.

The trend of the thermal conductivity, which is of much greater technical importance, as a function of the metal concentration at T = 100°C is shown in Fig. 12. Again the same sequence applies. It can be seen that 20 vol.% well-distributed chromium is already sufficient to approximately double the thermal conductivity compared to UO_2. The dependence on the Cr-content of the UO_2/Cr-cermets over the entire concentration range is shown in Fig. 13. The function has a S-shaped trend; the value for pure Cr was derived from literature [6].

Fig. 14 shows the temperature dependence of the thermal conductivity for UO_2, a few matrix metals and the corresponding UO_2/20 vol.% metal-cermets. The figure indicates, for example, that a UO_2/20 vol.% Cr cermet has a better thermal conductivity by about one order of magnitude than pure UO_2 at 800°C.

4. Fuel Pin Specimens for Irradiation Experiments

For the specifications of fuel pin specimens for irradiation experiments, the fast neutron absorption cross section of the matrix metals represents a decisive criterion. These values are listed in Table 1 for a few matrix metals. According to these data, only Cr and V are suited as matrix metals for fast reactors with high coolant temperatures. A few preliminary experiments with a molybdenum matrix had the result that only Cr and V were used.

Table 1.--Fast and thermal neutron absorption cross sections of a few matrix metals.

Matrix	$\sigma n\gamma$ (100KeV) (mb)	$\sigma n\gamma$ (therm) (barn)
Cr	6,8	3,1
V	9,5	15,1
Mo	71,0	2,7
Nb	100,0	1,15
SS1613	8,34	-

In selecting the cladding, only materials with a high heat and oxidation resistance could be considered for the high cooling gas temperature of a gas-cooled fast breeder. Thus, Inconel 625 and Hastelloy X were chosen for the UO_2-Cr cermets with a high target burnup. The material combinations, cladding materials and fabrication conditions are shown in Table 2.

Table 2.--Cermet fabrication conditions.

No.	Cermet/cladding	Specimen geometry Length x diam. x Cladding thickness (mm)	No. of specimens	Metal content (V/o)	Density (%th.)	Hot-bonding conditions Pressure (at)	Hot-bonding conditions Temp. (°C)	Holding time (h)
A	UO_2-Mo Niob	62x7,1x0,3	8	20 Mo	75	700	1260	4
B	UO_2-Cr Niob	62x7,1x0,3	8	30 Cr 20 Cr	90 83	500 400	1360 1300	4 4
C	UO_2-Cr Incoloy 800	62x6,3x0,4	8	30 Cr 20 Cr	92,5 90	450	1200	3
D	UO_2-Cr Inconel 625 Hastelloy X	105x8,4X0,4	4	30 Cr 20 Cr	83 80	150	1200	2
E	UO_2-Cr Inconel 625 Hastelloy X	105x8,3x0,4	4	30 Cr 20 Cr	80 78	150 200	1200	2
F	UO_2-V Vanadium	105x8,2x04	4	20 V	85-90	210	1300	2
	UO_2-V Vanadium	105x8,2x0,4	4	30 V 20 V	85 86	210 400	1300 1300	2

5. Irradiation Conditions

The irradiations were performed in the FR 2 at thermal neutron fluxes between 6 and $8 \cdot 10^{13}$ $n/cm^2 \cdot s$. The most important irradiation conditions and material data of the specimens are listed in Table 3. The mean linear rod power ranged between 450 and 700 W/cm at mean cladding temperatures of about 600°C. The maximum rod power and cladding temperature values were sometimes considerably higher. The maximum burnup amounted to 95.6 MWd/kg U with the use of UO_2/Cr fuel pins in an irradiation experiment.

The experiments were performed in a Na/K filled capsule (internal designation "capsule type 5a"). Fig. 15 shows a schematic diagram of such a capsule with a cermet fuel pin. The irradiation specimen

Table 3.--Material data and irradiation conditions of the cermet fuel pins

Fuel	UO_2-Mo	UO_2-Cr														UO_2-V*		
Device No.	A	B	C				D				E					F	G	
Metal concentration Vol.-%	20	20	20			30	20		30		20		30			20	20	30
Cladding material	Nb	Nb	Nb	Incoloy 800		Inconel 625	Inconel 625		Hastelloy X		Hastelloy X		Inconel 625			V	V	V
Wall thickness, mm	0,4	0,4	0,4	0,4	0,4	0,4	0,5	0,5	0,5	0,5	0,5	0,5	0,5	0,5		0,5	0,5	0,5
No. of specimens	8	8	1	3	3	1	1	1	1	1	1	1	1	1		4	2	2
Specimen diameter, mm	6,4-6,9	6,4-6,9	7,0	6,3	6,3	6,3	8,4	8,4	8,3	8,3	8,3	8,3	8,3	8,3		8,1-8,3	8,3	8,3
Specimen length, mm	62	62	62	62	62	62	116	116	116	116	116	116	116	116		116	116	116
Specimen density, % TD	75,85, 100	90,93	80	90	92,5	92,5	80	83	80	83	79	81	78	79		84-90	84,87	85
UO_2- weight, g	ca.9,8	ca.9,8	9,86	ca.6,4	ca.5,9	5,90	26,35	23,06	26,05	23,10	26,12	22,47	25,84	22,71		ca.23	ca.23	ca.21
Irradiation time, d	60	38	100	100	100	100	226	226	226	226	395	395	395	395		189	100	100
Burnup, MWd/kg U	14[1]	10[2]	31,1[1]	31[1]	33[1]	34,7[1]	60,2[1]	60,9[1]	58,2[1]	60,6[1]	84,8[1]	93,7[1]	95,6[1]	89,3[1]		55[1]	18[2]	19[2]
Rod power, W/cm																		
mean	550	500	560	450	450	460	670	640	600	595	535	510	600	490		715	450	435
maximum	600	580	600	500	500	600	800	730	690	670	710	640	740	630		800	600	610
Cladding temp., °C																		
mean	635	590	650	450	430	405	550	565	685	585	600	550	565	550		700	550	535
maximum	685	665	685	500	500	515	690	655	775	655	770	680	710	690		815	700	715

1) Determined by radiochemical methods.
2) Calculated according to thermal data.

has a threaded bolt at one end and a threaded sleeve at the other. These serve to bolt several specimens together into a set. This is located in a eutectic Na/K melt in a stainless steel inner capsule. The specimens are centered by thin perforated ribbed rings located between individual specimens. These rings also serve to guide the thermocouple immersion tubes. The temperature test points, a total of ten, are located at different axial positions in Na/K. The inner capsule in turn is inserted into an outer capsule of Zircaloy 2 filled with a eutectic Pb/Bi alloy. The irradiation device is located in the cooling water flow of the FR 2.

6. Post-irradiation Studies

After irradiation, the experimental devices were dismantled in the hot cells of the reactor plant and post-irradiation studies were performed. The capsule was first drilled and tested for fission gas that might have escaped from the specimens. After removal of the specimens they were inspected visually. Fig. 16 shows the four UO_2/Cr specimens of irradiation device E after irradiation. After the visual inspection the pins were subjected to an x-ray coarse structure study in the Betatron and to check the γ-activity over the fuel axis, a γ-scan was made. Fig. 17 shows such a γ-scan. The length and diameter of the specimens were determined in the dimensional control. The diameter was determined by a helical profilometer recording. Fig. 18 shows the helical profilometer tracings of a UO_2/Cr fuel pin before and after irradiation up to a burnup of 93.7 MWd/kg U. The diameter before and after irradiation is identical within a measuring error of $\pm$ 0.02 mm.

After the nondestructive tests, the specimens were drilled to determine the amount of fission gas released from the fuel. After aspirating the fission gases, the quantity was determined by gas chromatography. In order to determine bound fission gases, the fuel specimens were milled. Fission gas released during the milling process originates from pores in the fuel and is therefore called pore fission gas. The milled fuel was subsequently dissolved in acid. This released the remaining fission gas present in the fuel. It is called the matrix fission gas. In UO_2 it is present in dynamic solution and very small bubbles. For structure investigations, samples were taken at different sites of the specimens to prepare

axial and transverse microsections. Samples were also taken for radiochemical burnup analyses performed by determining Ce/Pr-144 as the burnup indicator at the Institute of Radiochemistry.

7. Results of Post-irradiation Studies

7.1 UO_2/Mo Cermets

A detailed report has already been made on the irradiation properties of these cermets [12]. Only the most important results will be repeated here. The Nb-cladded eight specimens of this irradiation device contained 20 vol.% Mo and were irradiated at 550 W/cm mean rod power and 635°C mean cladding temperature up to a burnup of 14 MWd/kg U. The cermet densities amounted to 75, 85 and almost 100% TD.

The pins with 75 and 85% TD showed a diameter increase of approximately 0.85% after irradiation. In the specimens with nearly 100% TD, a mean diameter increase of 1.5% was found. On the basis of the external dimensional changes, a mean swelling rate of 1.3 vol.%/% U burnup was calculated for the fuel of 75 and 85% TD and 1.7 vol.%/% U burnup for the high-density specimens. While the Nb claddings of the specimens of 75 and 85% TD remained free of cracks, those of the high-density specimens showed cracks with a primarily axial direction. The low elongation at fracture of Nb may be attributed to embrittlement by oxygen absorption from contaminated He during fabrication by hot-pressing. The cladding cracks partly continue into the fuel. Such macrocracks did not appear in the lower-density specimens.

Fig. 19 shows the structure of the specimens of various densities after irradiation. In the 75% TD specimen, some of the UO_2 particles show diametric cracks. The Mo coating around the UO_2 spheres, which often consists only of one particle layer, also exhibits frequent cracks. These cracks are caused by thermal stresses in the particles due to the very nonuniform thermal flux in this highly porous structure. The cracks disappear with increasing density. The high-density specimens exhibit practically no microcracks.

On the basis of these irradiation results, it was concluded that the optimum cermet density must be about 85% TD.

7.2 UO_2/Cr Cermets

7.2.1 General remarks. With the exception of irradiation device B, specimens with 20 and 30% Cr and cladded with high-heat resistant

Fe/Ni and Ni alloys were irradiated. The eight specimens of device B had 20% Cr and Nb claddings. The irradiation characteristics of these specimens have also been fully discussed in [12]. They were irradiated up to a burnup of 10 MWd/kg U. All specimens ruptured because of the embrittled Nb cladding. In view of the low strength of the Cr matrix compared to that of the Mo matrix, a higher degree of swelling occurred in the UO_2/Cr cermets than in the UO_2/Mo cermets. It was estimated to be about 2 vol.%/% U burnup.

The specimens of the second UO_2/Cr irradiation device were irradiated to a burnup of about 32 MWd/kg U. Incoloy 800 served as the cladding material for six specimens and Inconel 625 and Nb each for one specimen. The Nb-cladded specimen originated from the charge of the first UO_2/Cr device. The mean rod power of this specimen amounted to 560 W/cm with a mean cladding temperature of 650°C. The specimen ruptured. The remaining specimens of this irradiation device, because of their smaller diameter, had only a mean rod power of 450 W/cm with a mean cladding temperature of 440°C. Under these relatively mild irradiation conditions, the specimens developed no cracks in the cladding and no diameter increase. The idealized cermet structure remained unchanged. The specimens with 20% Cr exhibited a greater cracking tendency than those with 30% Cr.

The last two UO_2/Cr devices which were clad with 0.5 mm thick Inconel 625 and Hastelloy X, respectively, and were irradiated up to burnups of 60 and 95 MWd/kg U, respectively, are of greatest interest and most informative. The mean rod power values ranged between 490 and 670 W/cm with mean cladding temperatures from 550 to 685°C. A maximum of 775°C was measured in Hastelloy X and of 710°C in Inconel 625.

All specimens of both devices were in good and undamaged external condition after irradiation. No damage was detected. No diameter change was found in any specimen within the measuring accuracy of ± 0.02 mm. Length changes also could not be observed. Thus, the Inconel 625 and Hastelloy X claddings proved to be sufficiently strong to conduct fuel swelling into the fabrication porosity.

7.2.2 Cladding leakage. When the capsules were drilled, fission gas was found in both cases--i.e. 34.82 cm^3 in capsule D (mean burnup of 60 MWd/kg U, mean rod power 625 W/cm) and 14.28 cm^3 in capsule E (mean burnup 91 MWd/kg U, mean rod power 535 W/cm). These findings

indicate that microcracks were present in the cladding of some specimens. With the exception of the Inconel 625 specimen of device E, the specimens with 20% Cr also revealed occasional microcracks on the inside cladding surfaces but without extending to the outer surface. The maximum crack depth in Inconel 625 amounted to 0.4 mm. In Hastelloy X a maximum crack depth of 0.2 mm was detected in specimen E 1. In the specimens with 30% Cr no such cracks were ever detected.

The burnup values determined by radiochemical analysis and listed in Table 4 will serve as an indication of the cladding seal.

Table 4.--Fission gas data of the UO_2/Cr irradiation device D.

Specimen	%Cr	Cladding material	$G_{o,27}$ [1] cm^3	F [2] cm^3	P [3] cm^3	G [4] cm^3	(F+P+G) cm^3	$G_{o,27}$ - (F+P+G) cm^3
D 1	20	Inc.625	37,989	4,112	19,027	3,429	26,568	11,421
D 2	30	"	33,978		20,141			
D 3	20	Hast.X	36,158	1,637	14,299	5,088	21,024	15,134
D 4	30	"	33,531	4,967	18,551	4,819	28,337	5,194
Capsule				34,82			Total	31,749 <34,82

1) Theoretical fission gas volume produced with 0.27 gas atoms/fission.
2) Free fission gas.
3) Pore fission gas.
4) Matrix fission gas.

The fission nuclides Ce-144 and Cs-137 served as burnup indicators. Ce and its daughter product Pr remain at the site of origin because Cs is volatile. Thus, the absence of Cs suggests cladding leakage. The burnup values of Table 5 then indicate that specimens D 1, D 3 and E 1 with 20% Cr and specimen E 2 with 30% Cr and a Hastelloy X cladding leaked. The Inconel 625-clad specimens E 3 and E 4 had not developed leaks according to these findings. No definite information is available for specimens D 2 and D 4. On the basis of the fission gas balance for device D (Table 4), however, it can not

be ruled out that these two specimens may not have also released small quantities of fission gas. The large quantity of fission gas found in the capsule of this device can only be explained by the assumption that at least specimen D 4 with 30% Cr and a Hastelloy X cladding has released fission gas. Specimen D 2 might have remained leak-free if at least 0.28 fission gas atoms were formed per fission event.

Table 5.--Burnup values determined by radiochemical analysis.

Device	Specimen	Burnup, MWd/kg U	
		Ce-144	Cs-137
D	1	60,2	39,0
	2	60,9	58,8
	3	58,2	48,9
	4	60,6	57,1
E	1	84,84	76,87
	2	93,73	69,62
	3	95,60	97,82
	4	89,34	95,28

On the basis of the quantities of free fission gas found in the specimens and the available free volume, fission gas pressures of 10-40 atm may be estimated to have been generated under the operating conditions near the end of irradiation. The maximum possible fission gas pressure (cladding cracks forming only near the end of irradiation) would be about 100 atm. No free fission gas was detected in specimens E 2, E 3 and E 4. In specimen E 2 this is attributable to leaks, while in specimens E 3 and E 4 the entire fission gas was evidently retained in the fuel. Thus, these specimens were not under a significant fission gas pressure.

7.2.3 Changes in structure. All four specimens with 20% Cr from irradiation devices D and E show demixing of UO_2 and Cr in the core which does not occur in the specimens with 30% Cr (Figs. 20 and 21). Cr has migrated outward under the influence of the temperature gradient, i.e. it evaporated in the interior at the warmer sites and condensed farther toward the outside in the colder zones. UO_2 remained

in the center and underwent a structural rearrangement by sintering of individual particles and pore migration, to the point that central channel formation even occurred in some cases (Fig. 21). The more extensive crack formation in specimens with 20% Cr is also apparent in Figs. 20 and 21.

Fig. 22 shows the structure developed in a specimen with 20% Cr after a burnup of 60 MWd/kg U as a function of the radius. Various zones can be distinguished in a direction toward the center:

The interface between fuel and cladding,

A zone with a nearly unchanged fuel structure in which only the porosity changed in the UO_2,

A Cr-enriched zone in which disruption of the idealized cermet structure begins with the penetration of Cr into the UO_2 particles along the grain boundaries,

The UO_2 zone from which Cr has almost completely evaporated.

Fig. 22 shows the structure of specimen E 2 with 30% Cr in the outer zone and the center after a burnup of 93.7 MWd/kg U. No significant structural differences are present between the outer zone and the center and only the pores in the UO_2 particles in the center are somewhat larger.

As a result of UO_2/Cr demixing in the specimens with 20% Cr, a greater release of volatile fission products which are responsible for cladding damage occurs in addition to greater fission gas release. Figs. 24 and 25 show such damaged zones on the Inconel 625 and Hastelloy X cladding of the 20% Cr specimens after a burnup of about 60 MWd/kg U. The maximum depth of the reaction zones amounts to 0.2 mm in both specimens, even though the temperature of Hastelloy X was about 100°C higher than that of Inconel 625. In the 20% Cr specimens of device E, only reaction layers of a maximum of 0.1 mm thickness were observed. The reasons for this might reside in the lower rod power of these specimens with the resulting lower release of volatile fission products as well as the lower cladding temperature during the last irradiation cycles. No specimens with 30% Cr from both devices exhibited significant cladding damage.

7.3 UO_2/V Cermets

Two devices, each with four specimens, were irradiated. The first (Device F) containing only specimens with 20% V, attained a mean burnup of 55 MWd/kg U with a mean rod power of 715 W/cm and a mean cladding surface temperature of 700°C. Irradiation of the

second device (G), containing two specimens with 20% V and two with 30% V, was stopped after a burnup of about 18.5 MWd/kg U because of thermocouple malfunction. The mean rod power up to this time amounted to 450 W/cm with a mean cladding temperature of 550°C. The remaining material and irradiation data are listed in Table 3. In both devices, the cladding material consisted of pure vanadium in the absence of tubes of suitable V alloys.

After irradiation it was found that the cladding of all specimens had cracked. Fig. 26 shows a transverse microsection of such a specimen. Compared to the Mo and Cr materials, the irregular distribution of the V-matrix caused by the fabrication conditions is remarkable. The reason for fracture of the V cladding was their embrittlement by oxygen absorption, presumably originating from the Na/K filling of the capsule during irradiation. Oxidation during fabrication is not likely since the specimens were bright after hot pressing.

Fig. 27 shows the coarse-grained structure of a V cladding with oxide precipitates on the grain boundaries.

Fig. 28 represents the structure at the outer zone and in the center of a UO_2/20% V specimen after a burnup of 54 MWd/kg U. The structure of the outer zone was not significantly influenced by irradiation. However, in the hotter zone, some pores can be seen in the V, evidently in the process of migrating toward the center. Compared to Cr, the migration rate is very slow due to the substantially lower vapor pressure of V. Signs of a forming central channel or notable UO_2/V demixing are not yet present.

8. Conclusions

On the basis of these experiments, a successful irradiation behavior of cermet fuel pins with an idealized structure requires the preservation of this structure. Demixing of ceramic fuel and matrix metal by metal evaporation in the center is not permissible because of the resulting increase in fission gas and volatile fission product release and the consequences of this release--buildup of an unpermissibly high fission gas pressure and weakening of the cladding by fission product attack.

An estimate of the maximum center temperature of the specimens with 20% Cr in irradiation devices D and E, in which UO_2/Cr demixing

was observed, resulted in values of between 1200 and 1300°C on the basis of the thermal conductivity of the unaffected cermet structure. With consideration of the influence of time, it is probable that the maximum permissible limit of the center temperature in UO_2/Cr cermets will have to be considered 1200°C. Consequently, cermets with 20% Cr are not suited for irradiation conditions of technical interest. With a Cr concentration of 30% and a cladding temperature of 650°C, a rod power of 800 W/cm must be viewed as the limit value with which burnups of at least 60 MWd/kg U can be realized. It would be possible to increase the rod power if a matrix metal of lower vapor pressure could be used. If the requirement for a small fast neutron capture cross section is taken into account at the same time, only V can be considered, although its disadvantage resides in its high oxygen affinity, so that its use in a U/Pu mixed oxide cermet would have to be ruled out.

Inconel 625 and Hastelloy X as a cladding material with a wall thickness of 0.5 mm are in the position to guide fuel swelling into the fabrication porosity and thus to maintain external dimensional stability. However, the question of microcrack formation has not yet been fully clarified. Inconel 625 proved useful up to mean temperatures of 565°C with maximum temperatures of 700°C if the cermet fuel contained 30 vol.% Cr. Hastelloy X proved to be more sensitive to microcracks, although it must be kept in mind that in both irradiation devices , the temperatures of the Hastelloy X claddings were up to 100°C higher than those of the Inconel 625 claddings.

Literature

[1] M. Dalle-Donne, S. Förster: Gas Breeder. Memorandum (Sept. 1970).

[2] M. Fischer: Feasibility study for the fast high-flux test reactor FR 3. KFK 1356 (March 1971).

[3] S. Nazaré, G. Ondracek, F. Thümmler: On the technology of cermets. High Temperatures - High Pressures 3, 615 (1971).

[4] V. B. Nesterenkow: Physical and technical parameters of the dissociating nitrogen tetroxide in nuclear power plants with gas-cooled fast reactors (Translation [from Russian to German]). Minsk, 1972.

[5] H. Schneider, D. Schönwald: Vapor deposition of molybdenum on zirconium oxide and uranium dioxide particles. KFK 555 (Jan. 1967).

[6] H. Schneider, D. Schönwald: Vapor deposition of chromium on UO_2- and Al_2O_3-particles. KFK 787 (July 1968).

[7] H. Schneider, D. Schönwald: Vapor deposition of V. KFK 1292 (Oct. 70).

[8] P. Weimar, F. Thümmler, H. Bumm: Fabrication and properties of cermets with idealized structure by isostatic hot pressing of coated particles. Second European Symposium on Powder Metallurgy. Stuttgart, May 1968 and J. Nucl. Mat. 31 (1969).

[9] P. Weimar: Fabrication and properties of cermets with idealized structure (UO_2/Mo and UO_2/Cr). Diss. 1969, TH Univ. Karlsruhe.

[10] H. Bumm et al.: Recent findings in the field of cermets with idealized structure by isostatic hot pressing of coated particles. Symp. on Fast Reactor Fuel and Fuel Elements, ANS, Karlsruhe (Sept. 1970).

[11] C. S. Swamy, P. Weimar: Electric Conductivity of Cermets with Idealized Structure between Room Temperature and 1000°C. Powder Met. Int. (1970).

[12] W. Dienst, P. Weimar: First irradiation experiments with UO_2 Mo and UO_2 Cr cermets with 80 vol.% UO_2 in Nb cladding. Karlsruhe Nuclear Research Center, External Report 6/69-1.

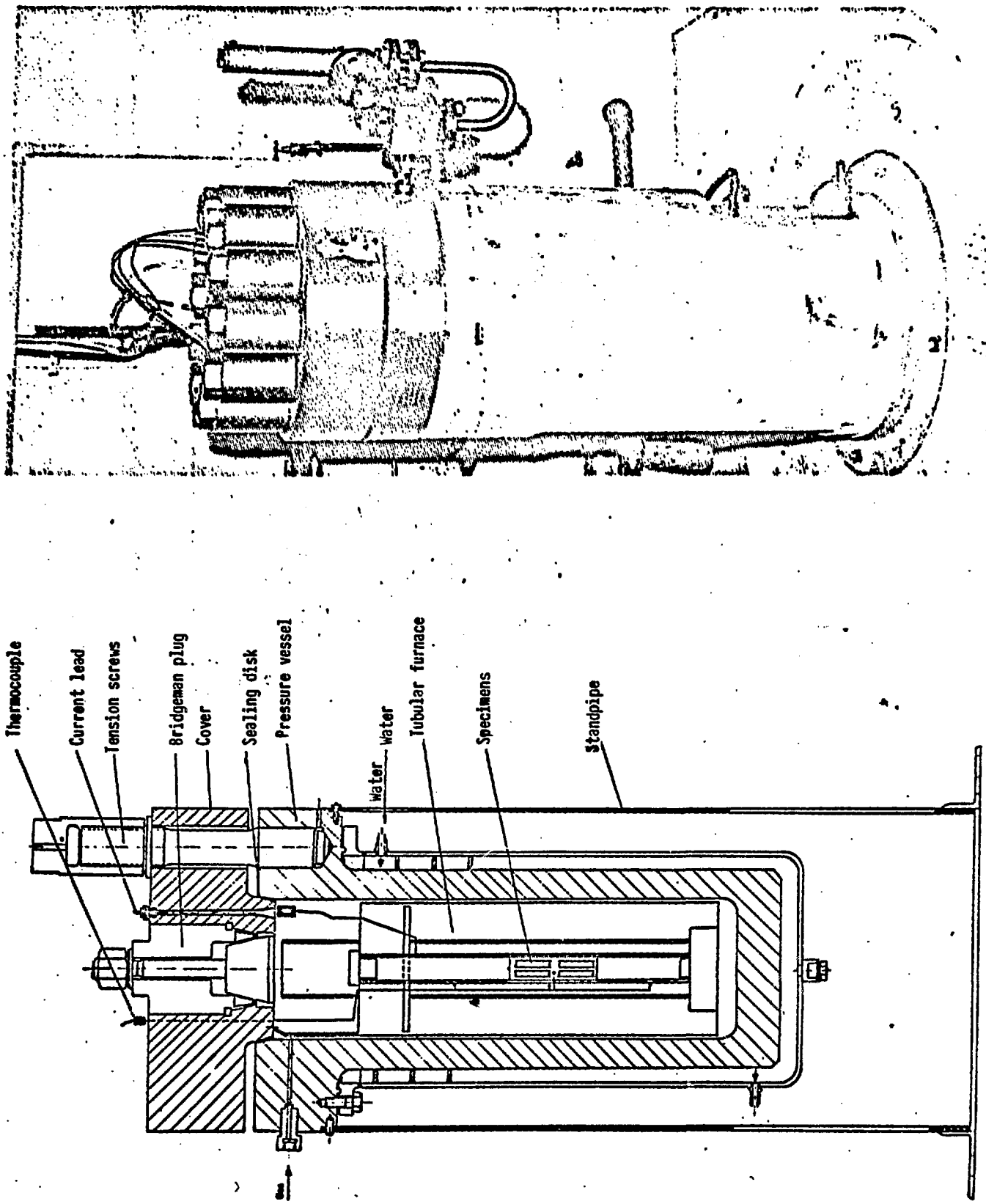

Fig. 1.--Cross section and view of the hot-pressing autoclave (manufacturer: UHDE).

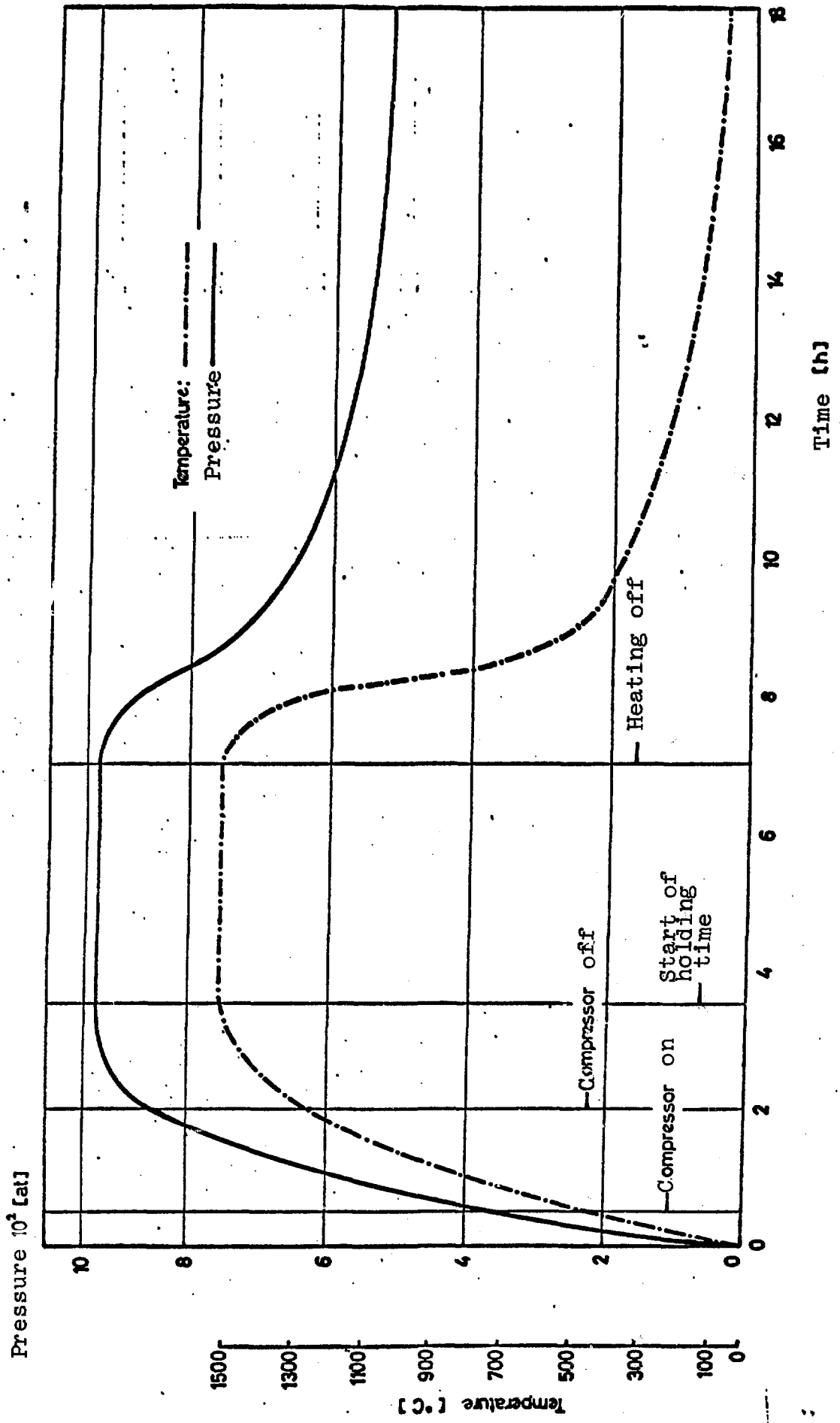

Fig. 2.--Pressure-temperature cycle for isostatic hot pressing.

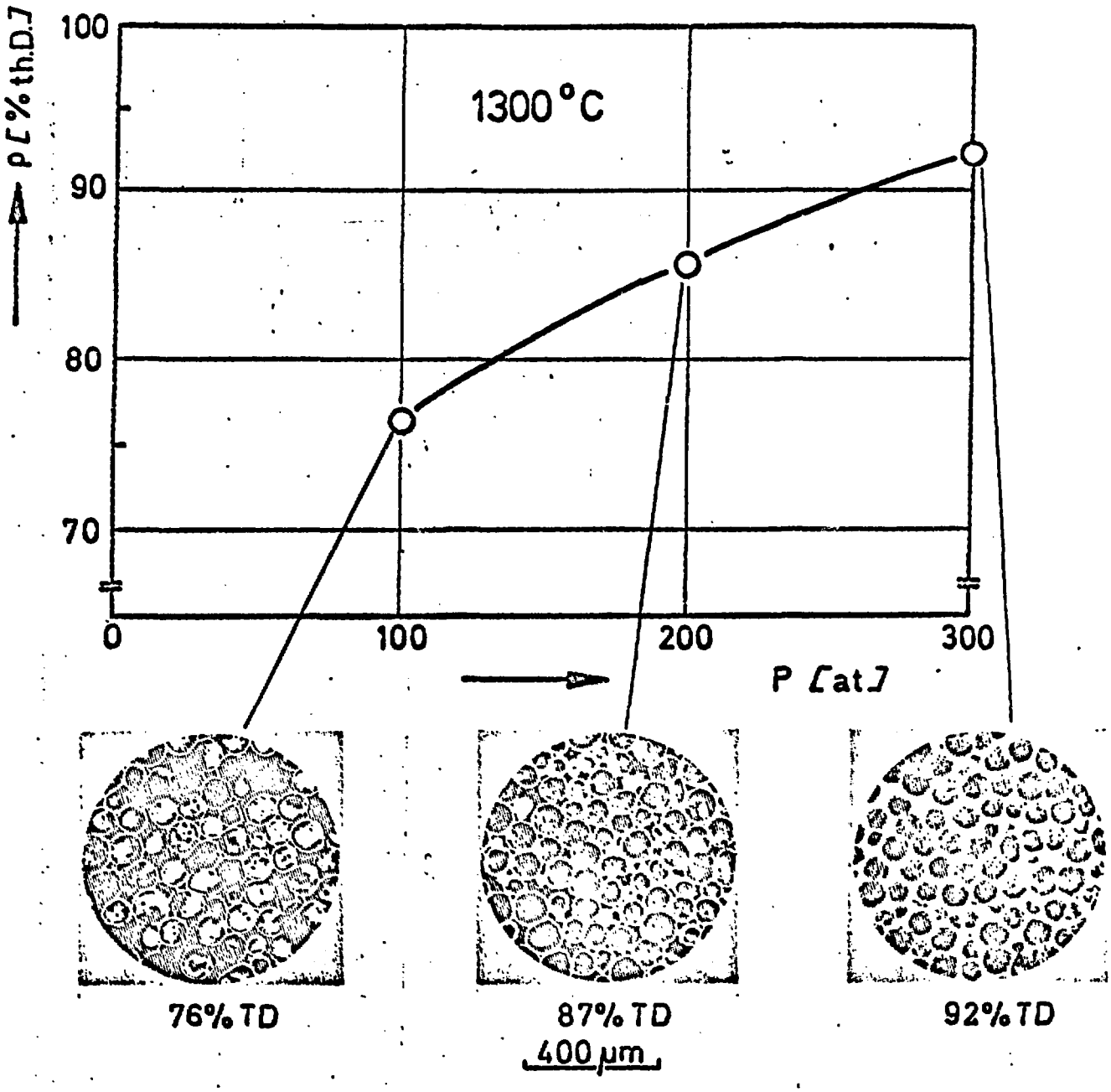

Fig. 3.--Density as a function of pressure for UO_2/30 vol.% Cr cermets.

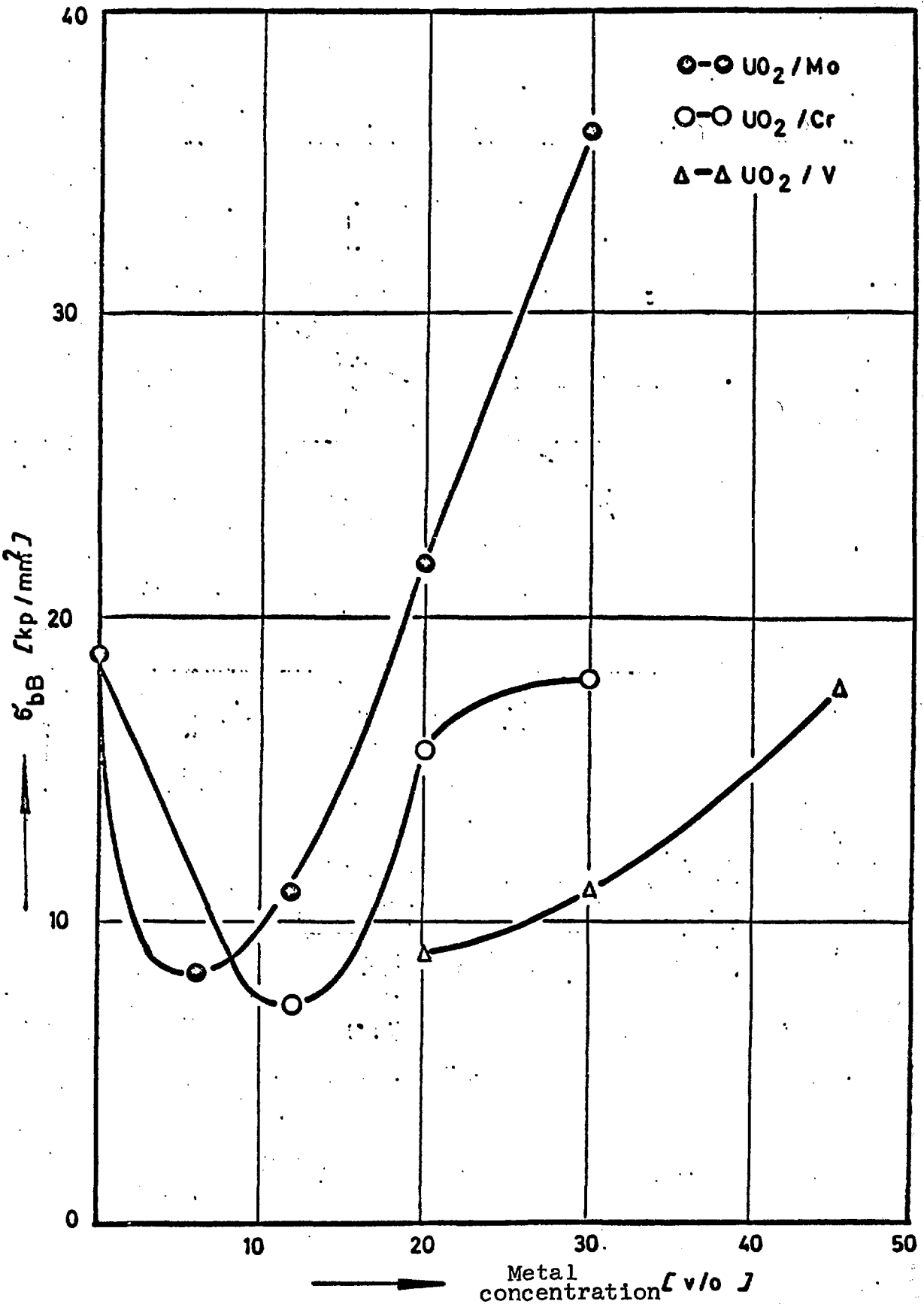

Fig. 4.--Bending strength as a function of the metal content for UO_2 (Mo,Cr,V)-cermets.

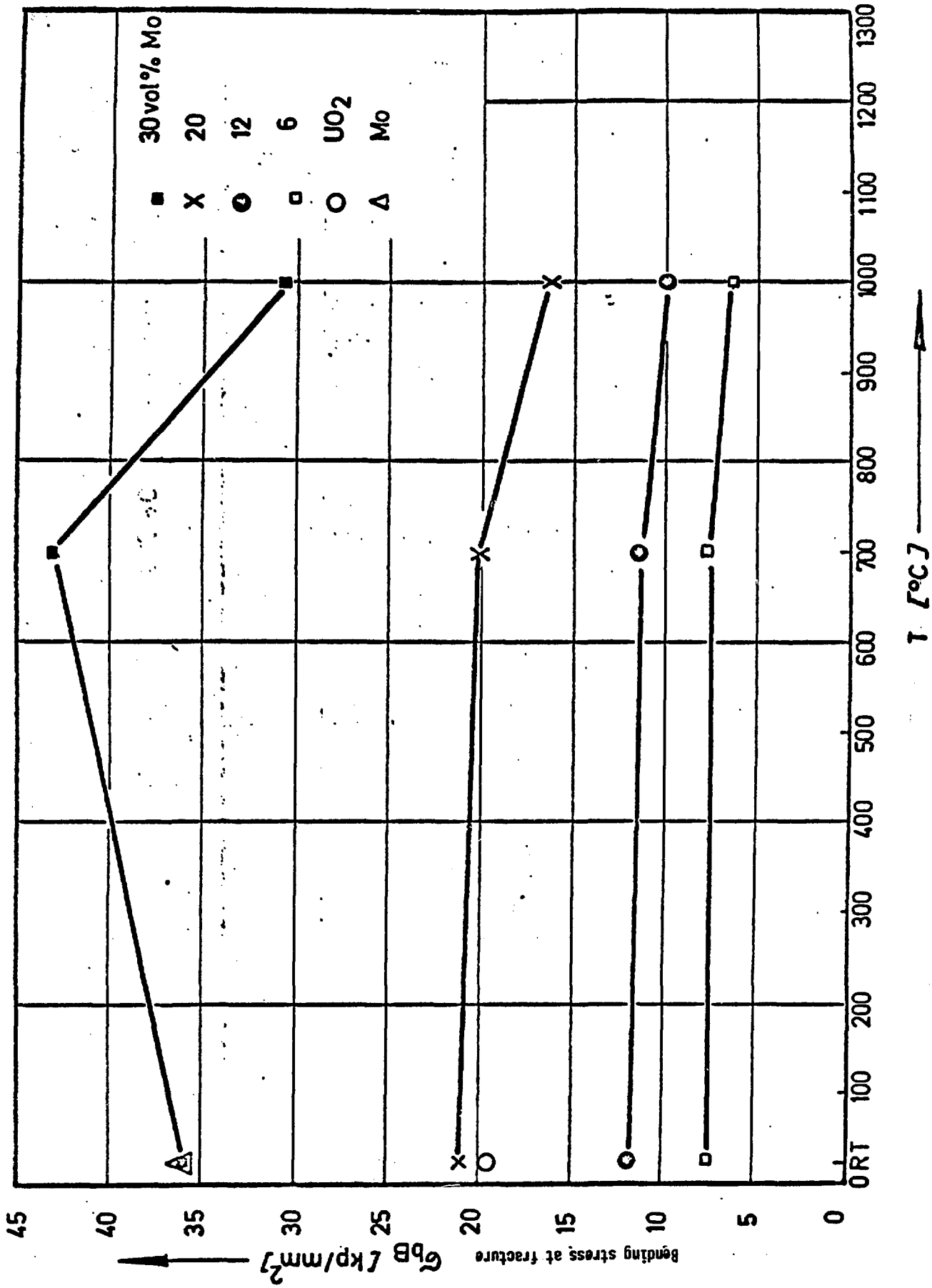

Fig. 5.--Bending strength as a function of temperature of some UO_2/Mo cermets.

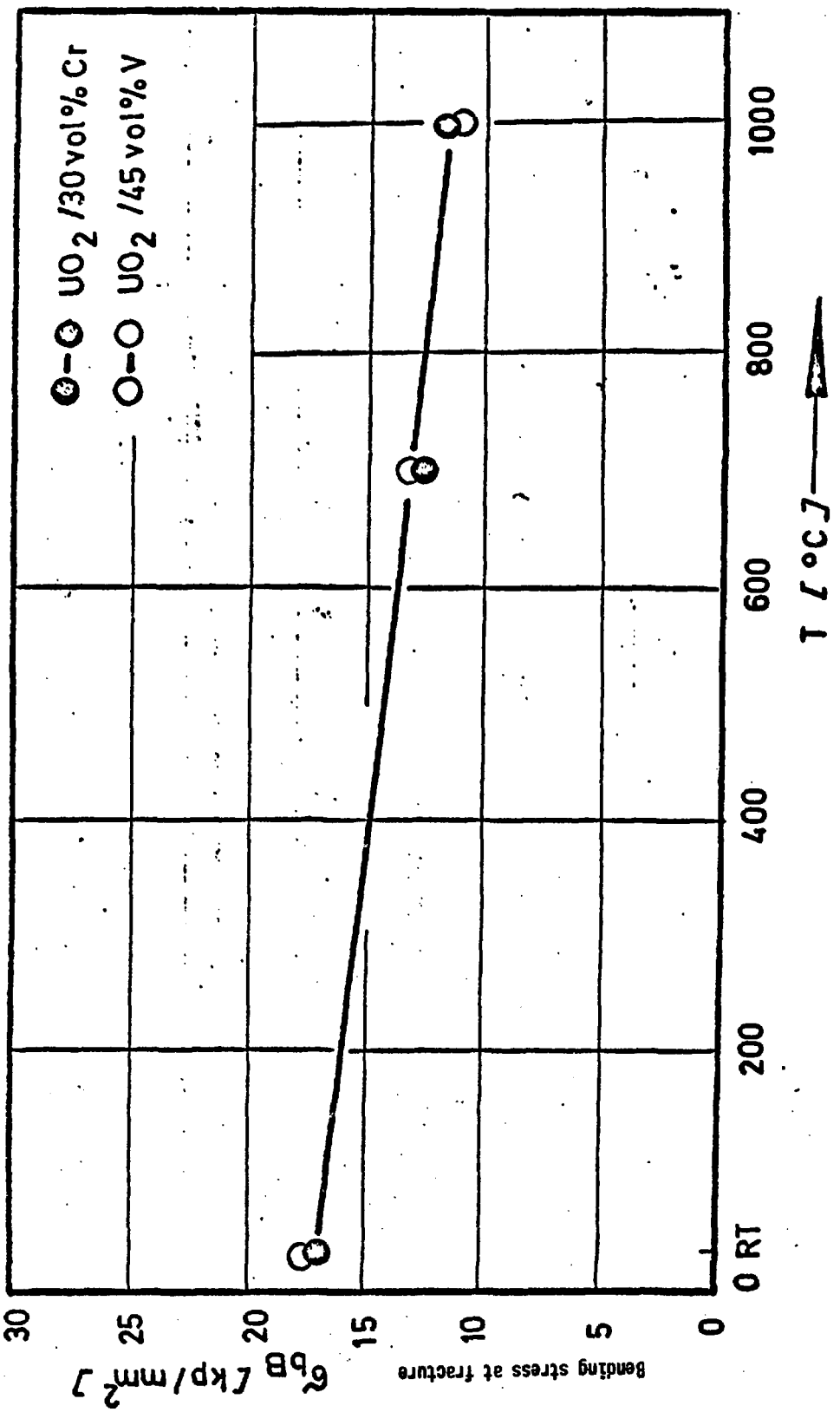

Fig. 6.--Comparison of the temperature-dependent bending strength of UO_2/30 vol.% Cr and UO_2/45 vol.% V cermets.

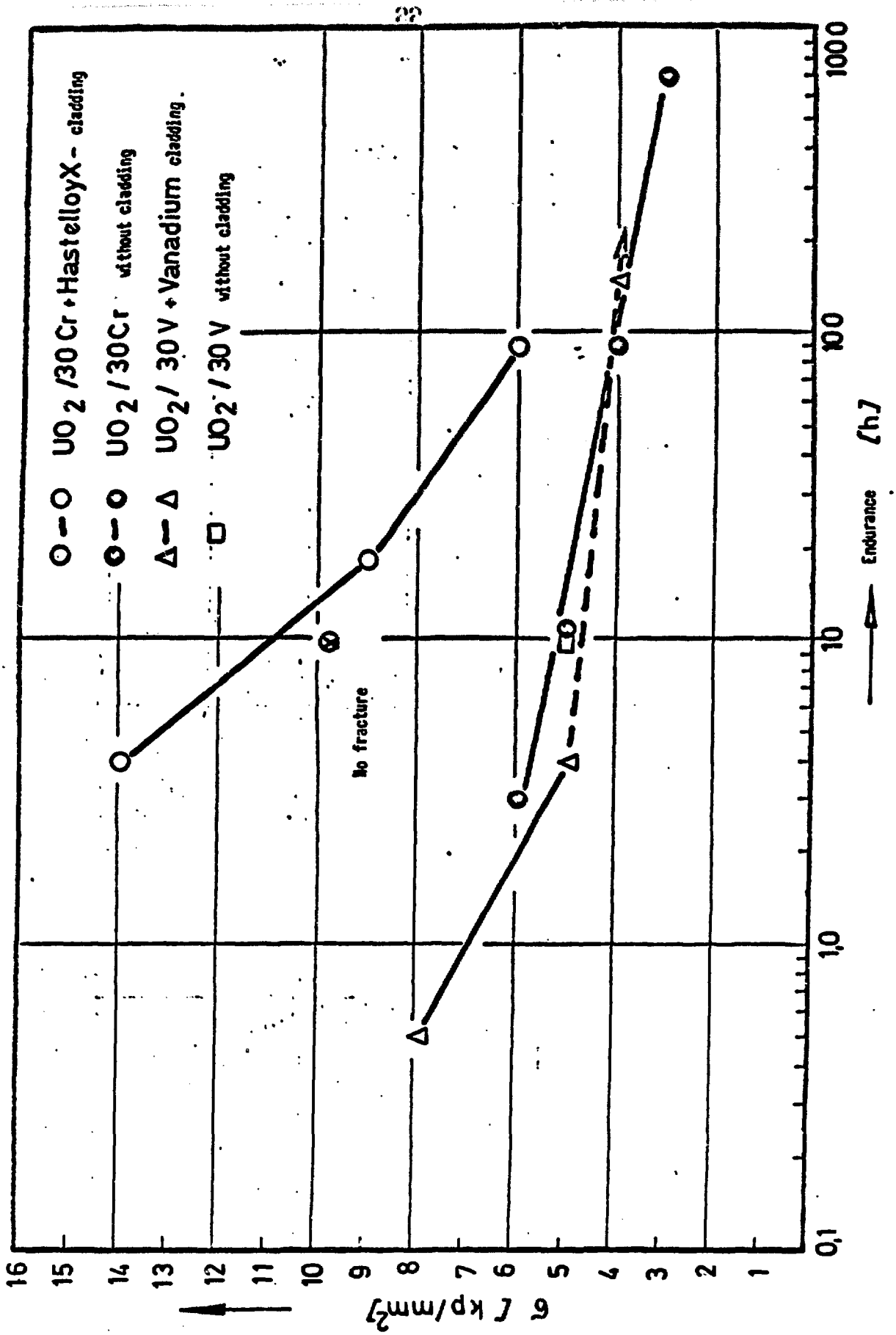

Fig. 7.--Endurance of clad and unclad UO_2/30 vol.% (Cr,V) cermets.

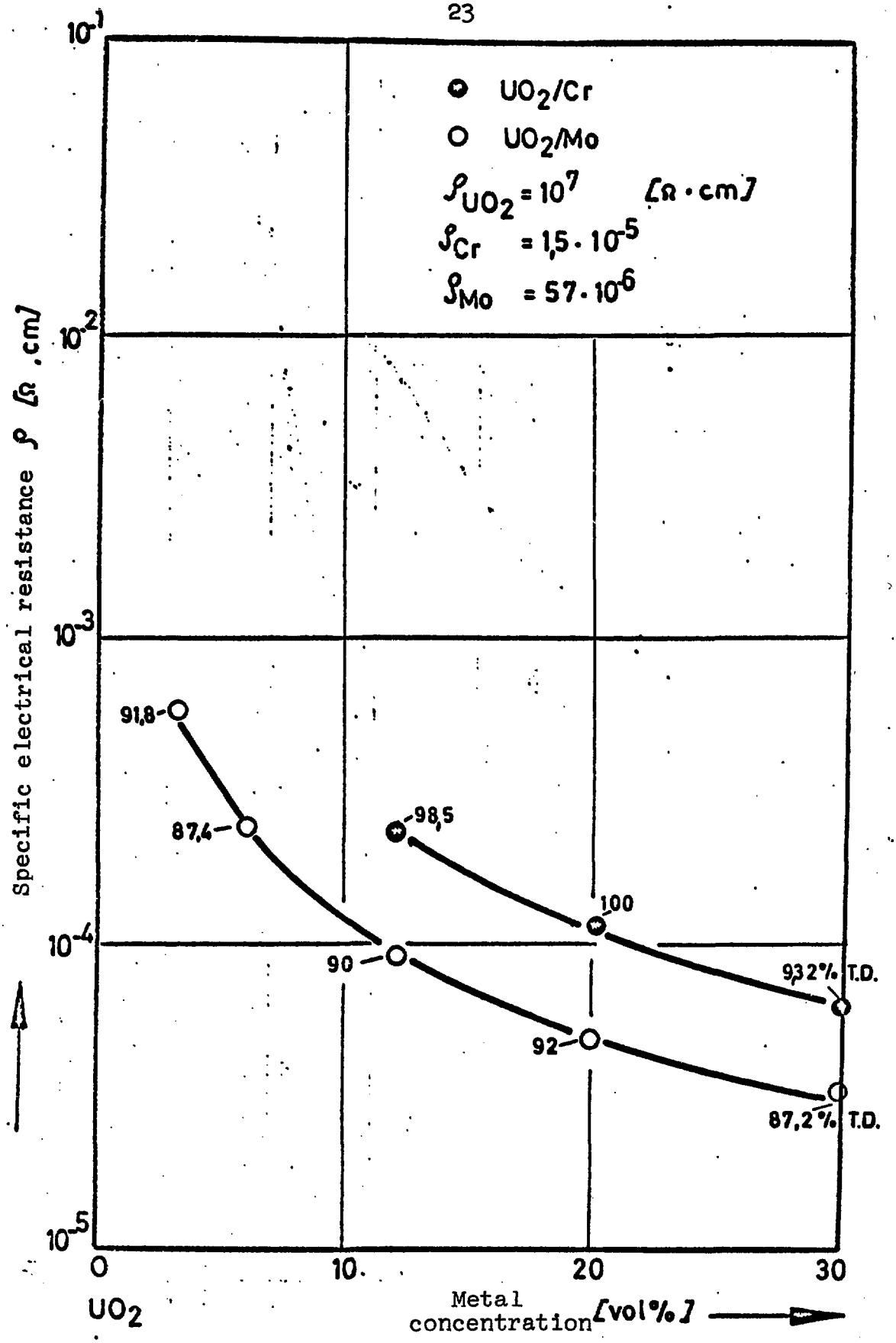

Fig. 8.--Specific electrical resistance as a function of metal concentration in UO_2/Mo and UO_2/Cr cermets.

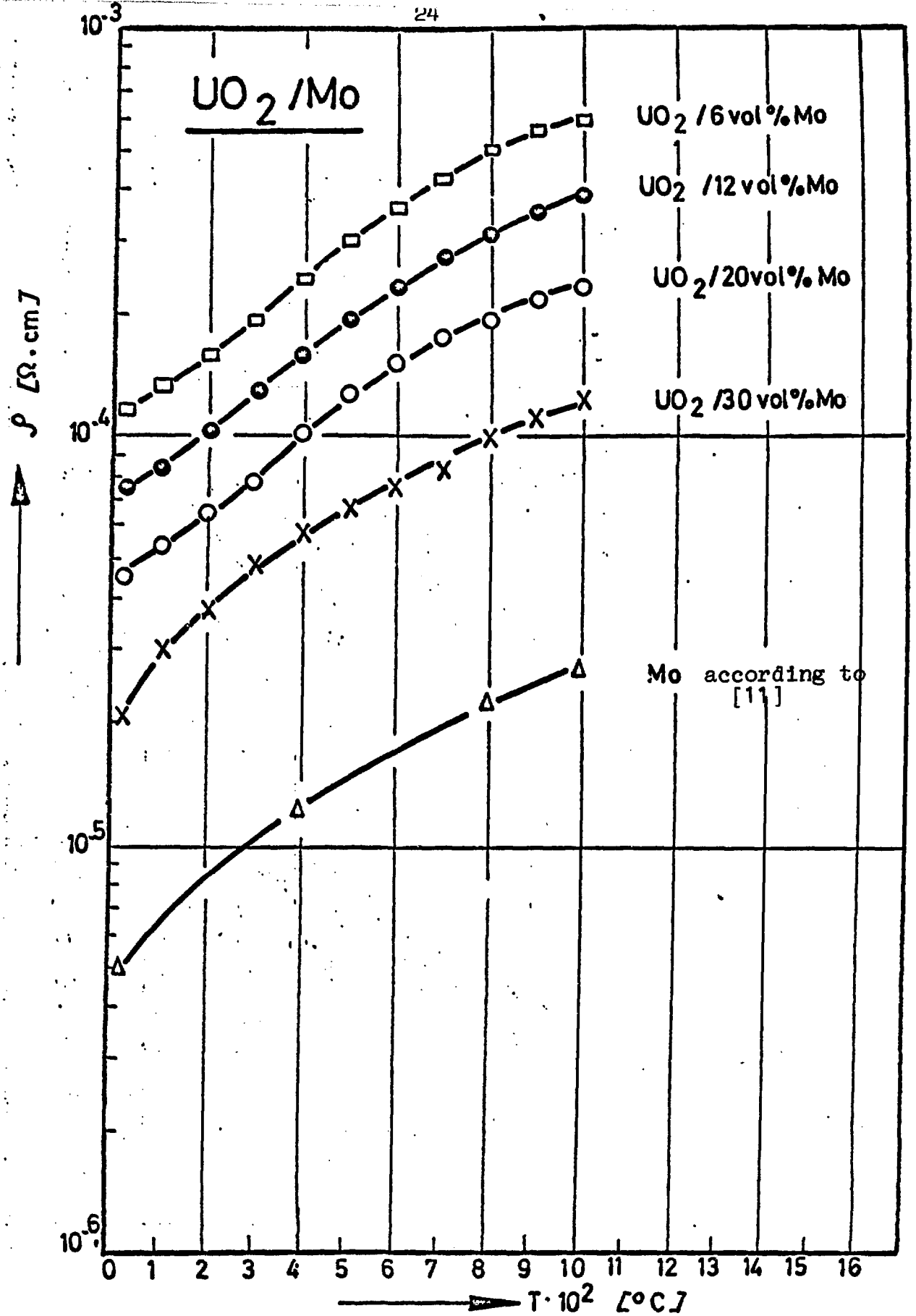

Fig. 9.--Temperature functions of the specific electrical resistance for idealized UO_2/Cr structures.

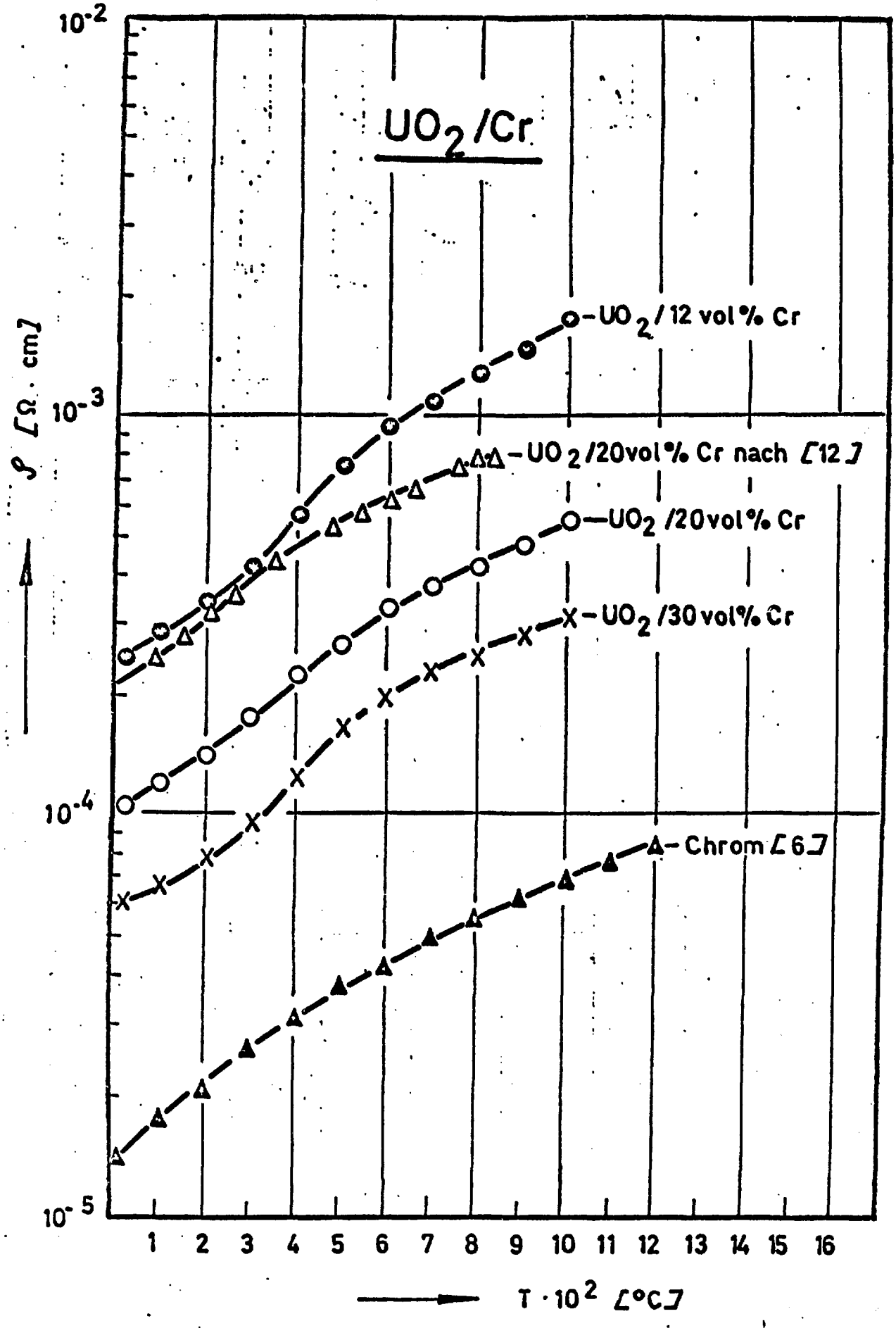

Fig. 10.--Temperature functions of the electrical resistance for idealized UO_2/Cr structures.

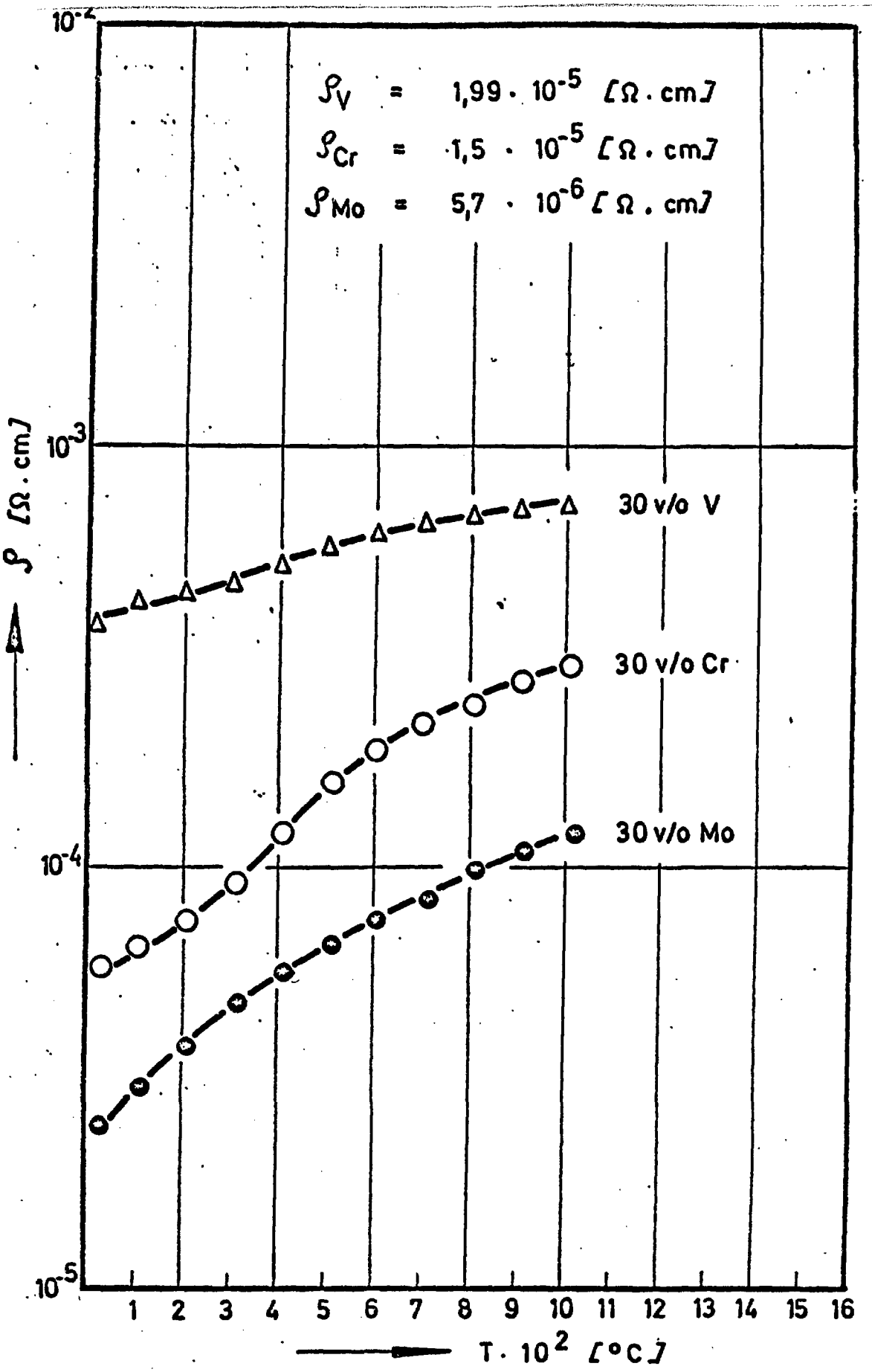

Fig. 11.--Comparison of the specific electrical resistance as a function of temperature for UO_2/30 vol.% (Mo,Cr,V) cermets.

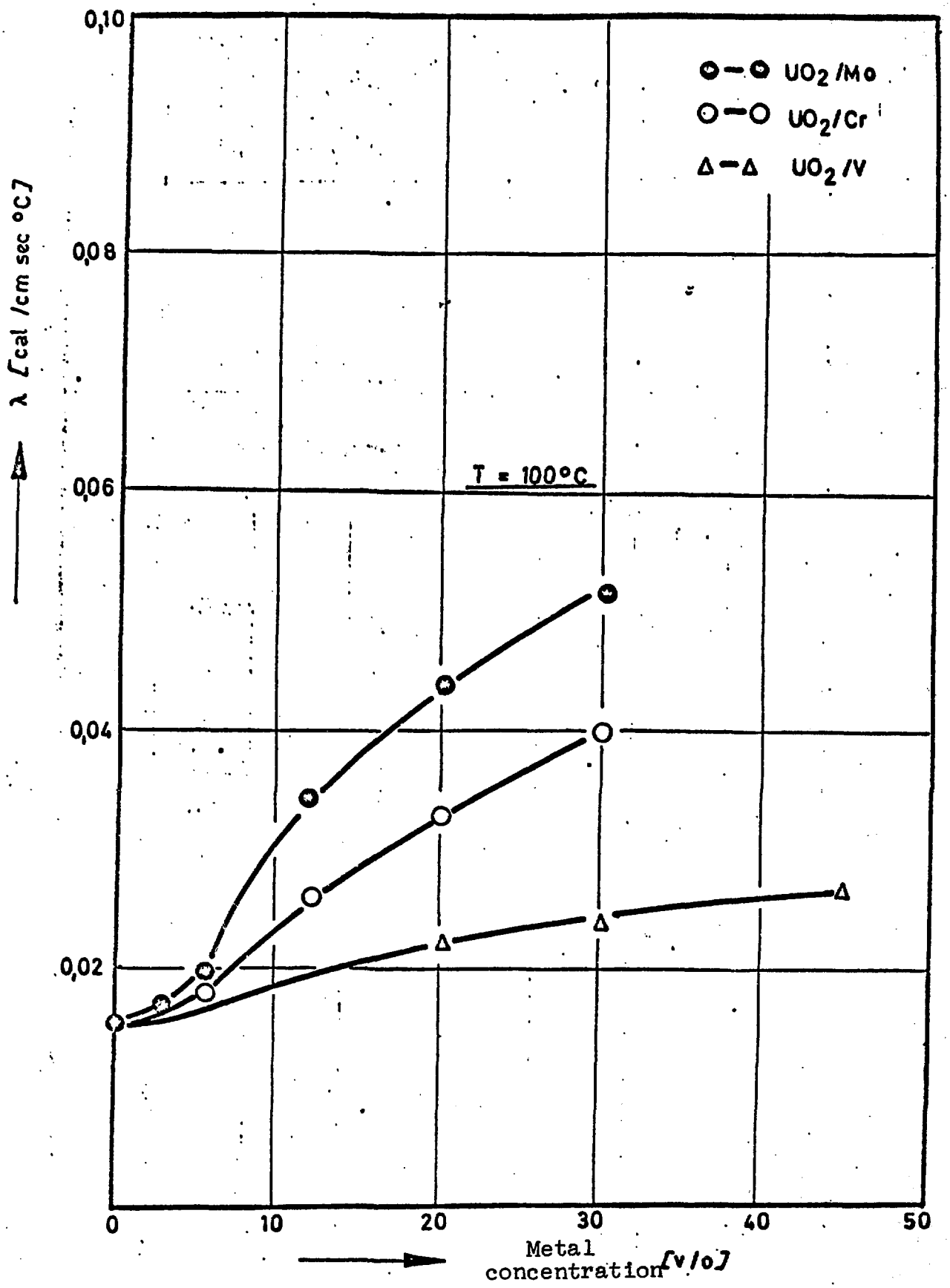

Fig. 12.--Thermal conductivity as a function of the metal concentration of UO_2/(Mo,Cr,V) cermets.

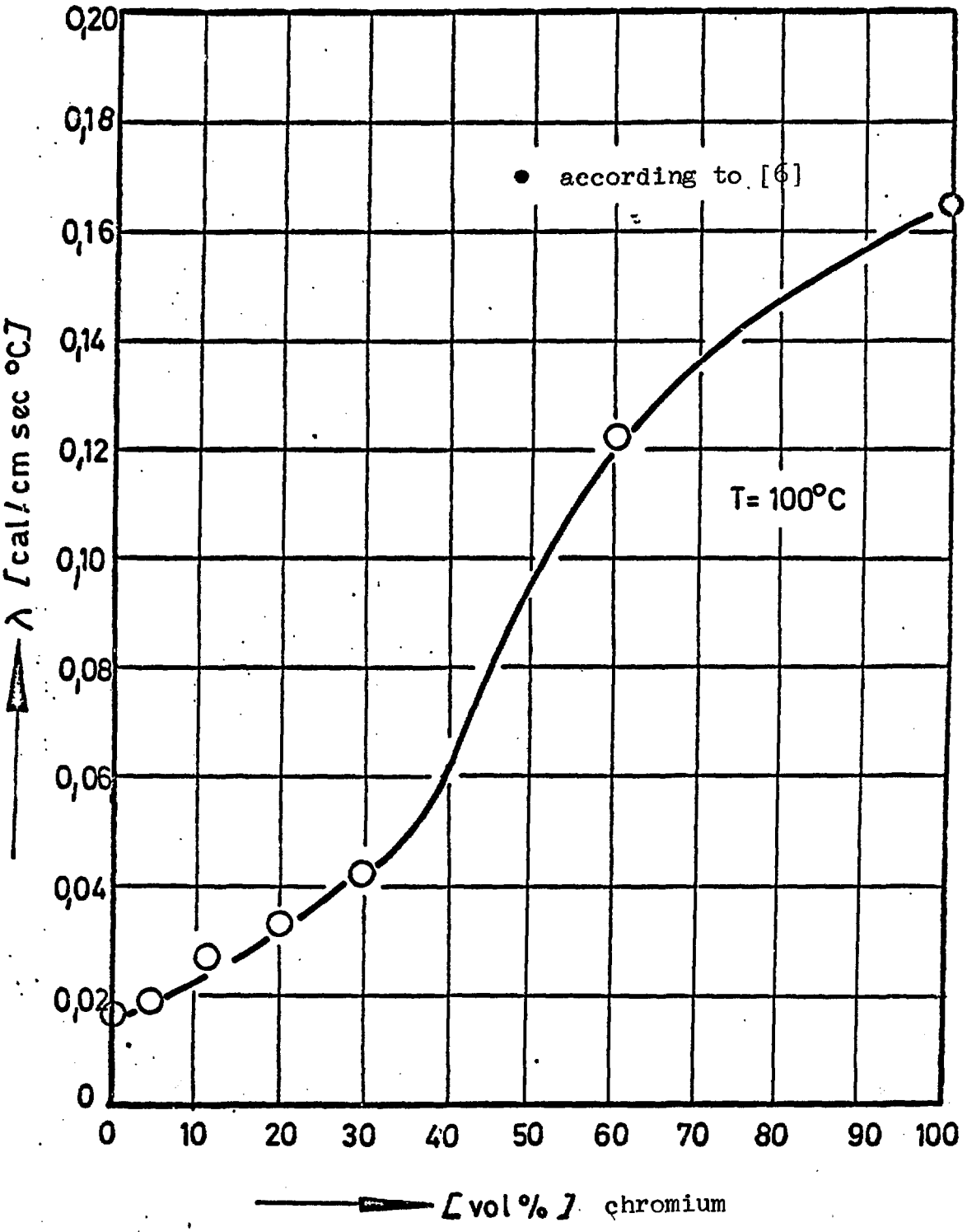

Fig. 13.--Thermal conductivity of UO_2/Cr cermets as a function of metal concentration at 100°C.

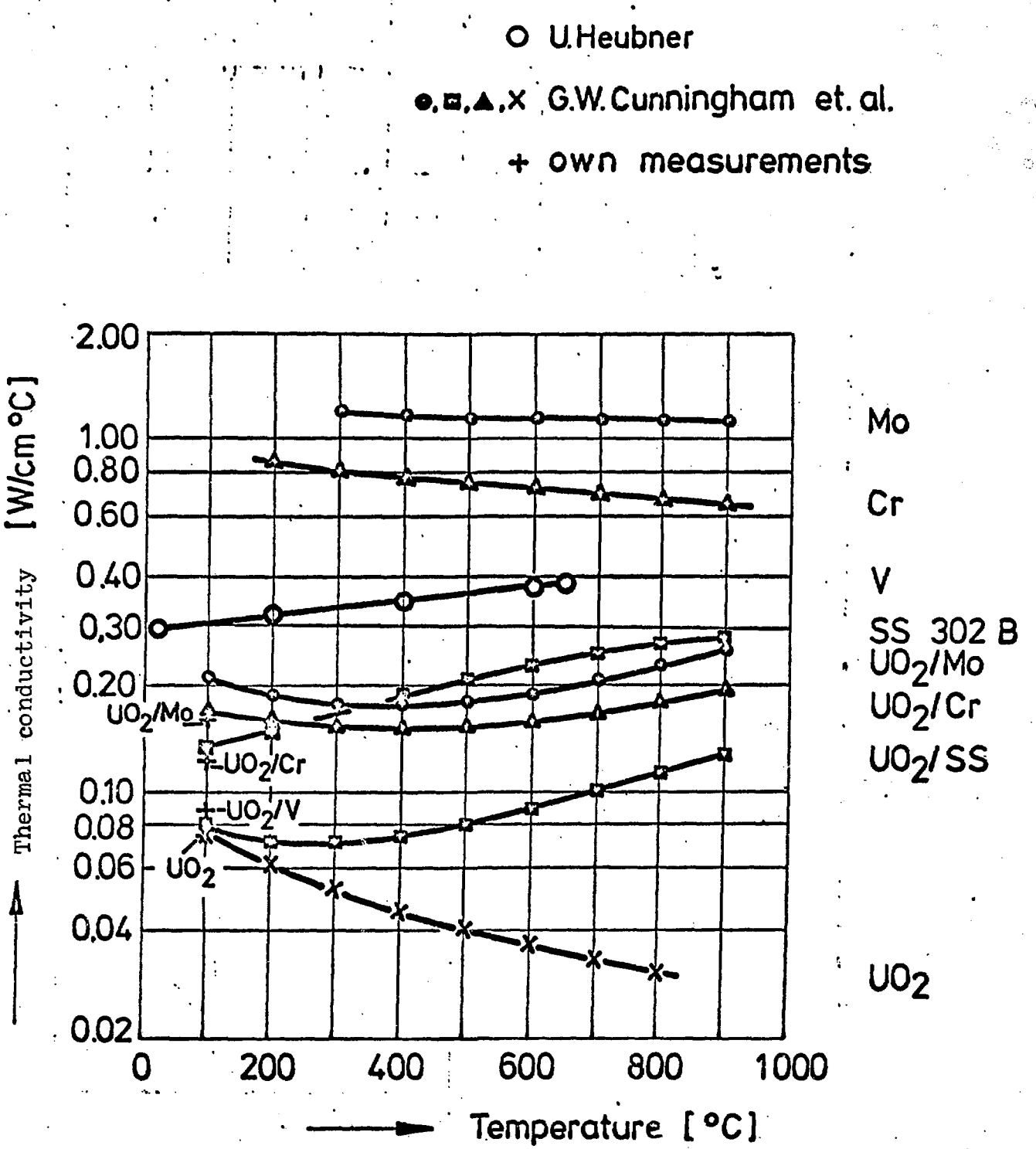

Fig. 14.--Temperature functions of the thermal conductivity for UO_2, some matrix metals and UO_2/20 vol.% metal cermets.

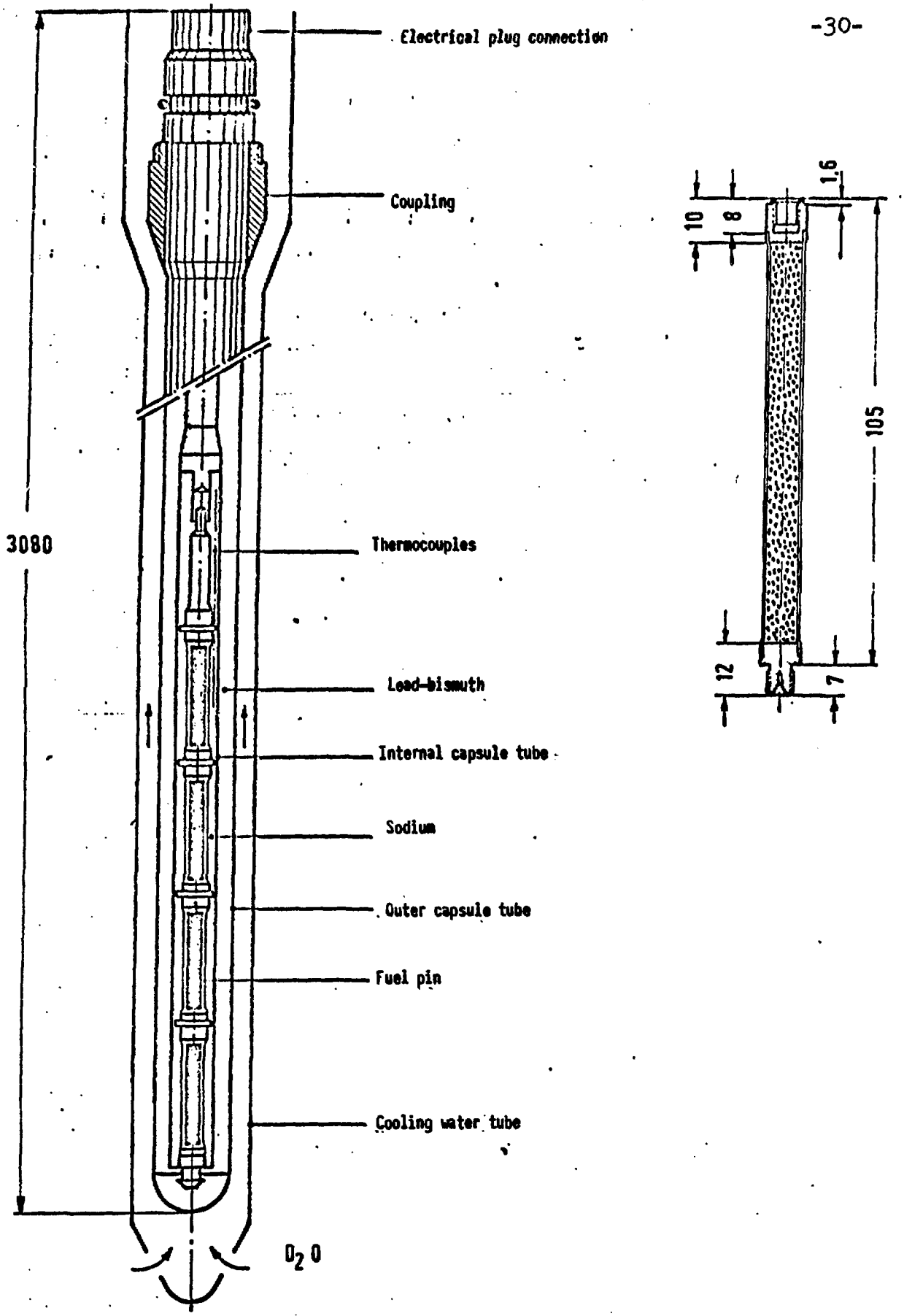

Fig. 15.--FR 2 irradiation capsule type 5a and cermet irradiation specimen--schematic diagram.

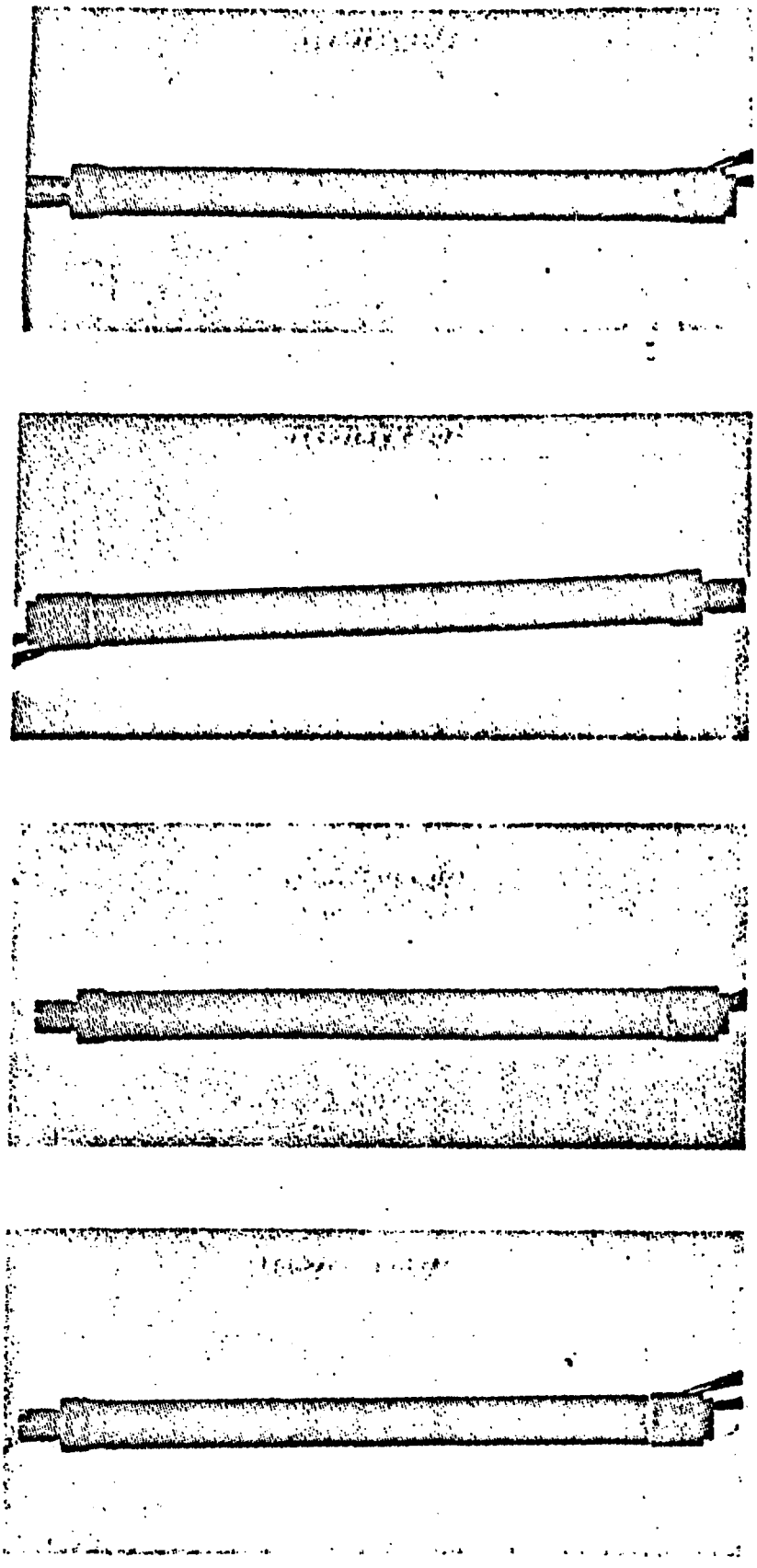

Fig. 16.--UO_2/Cr specimens of device E after irradiation. Burnup: 85-95 MWd/kg U.

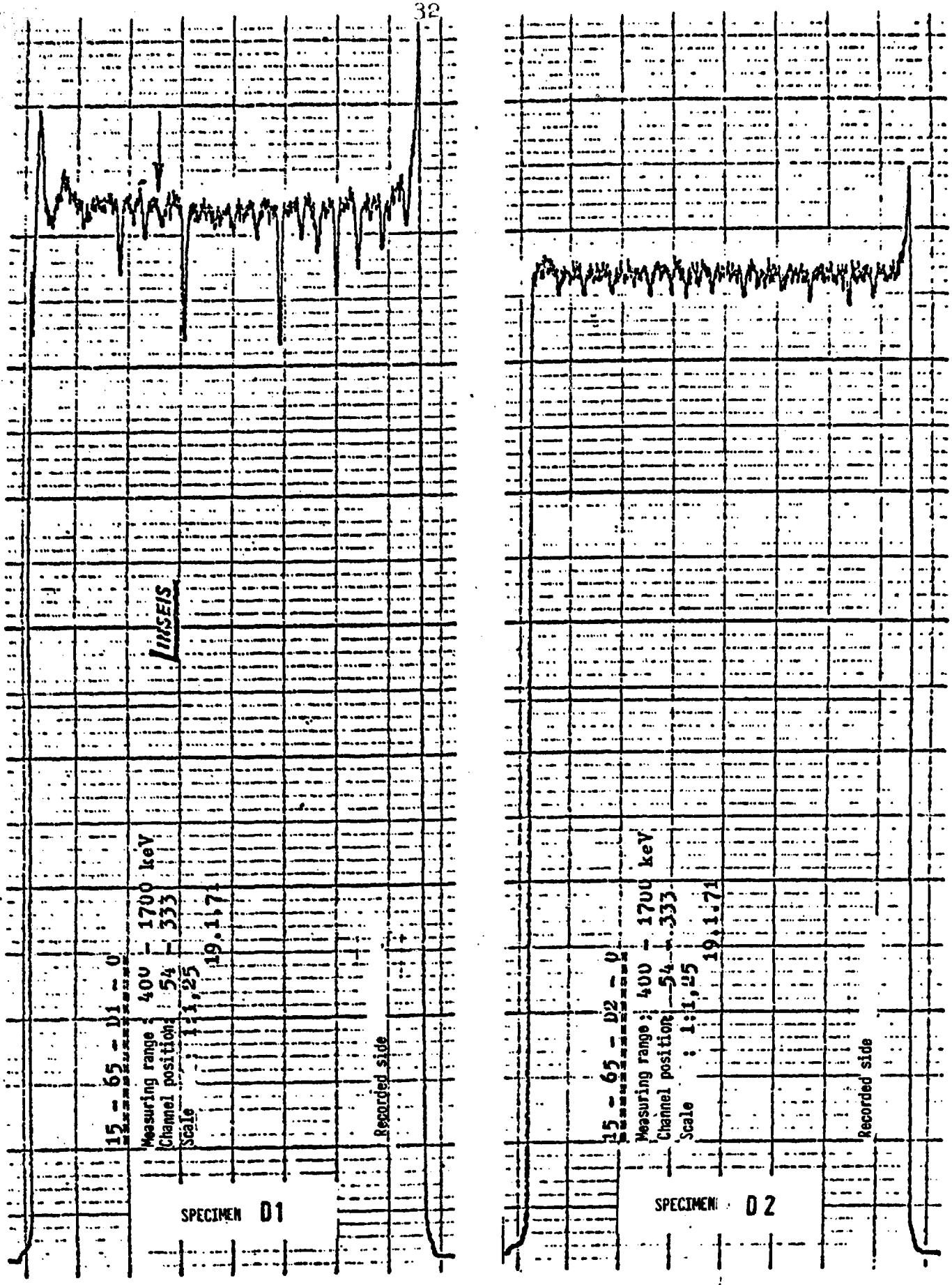

Fig. 17.--Integral γ-profiles of a UO_2/20% Cr specimen and a UO_2/30% Cr specimen after about 60 MWd/kg U burnup.

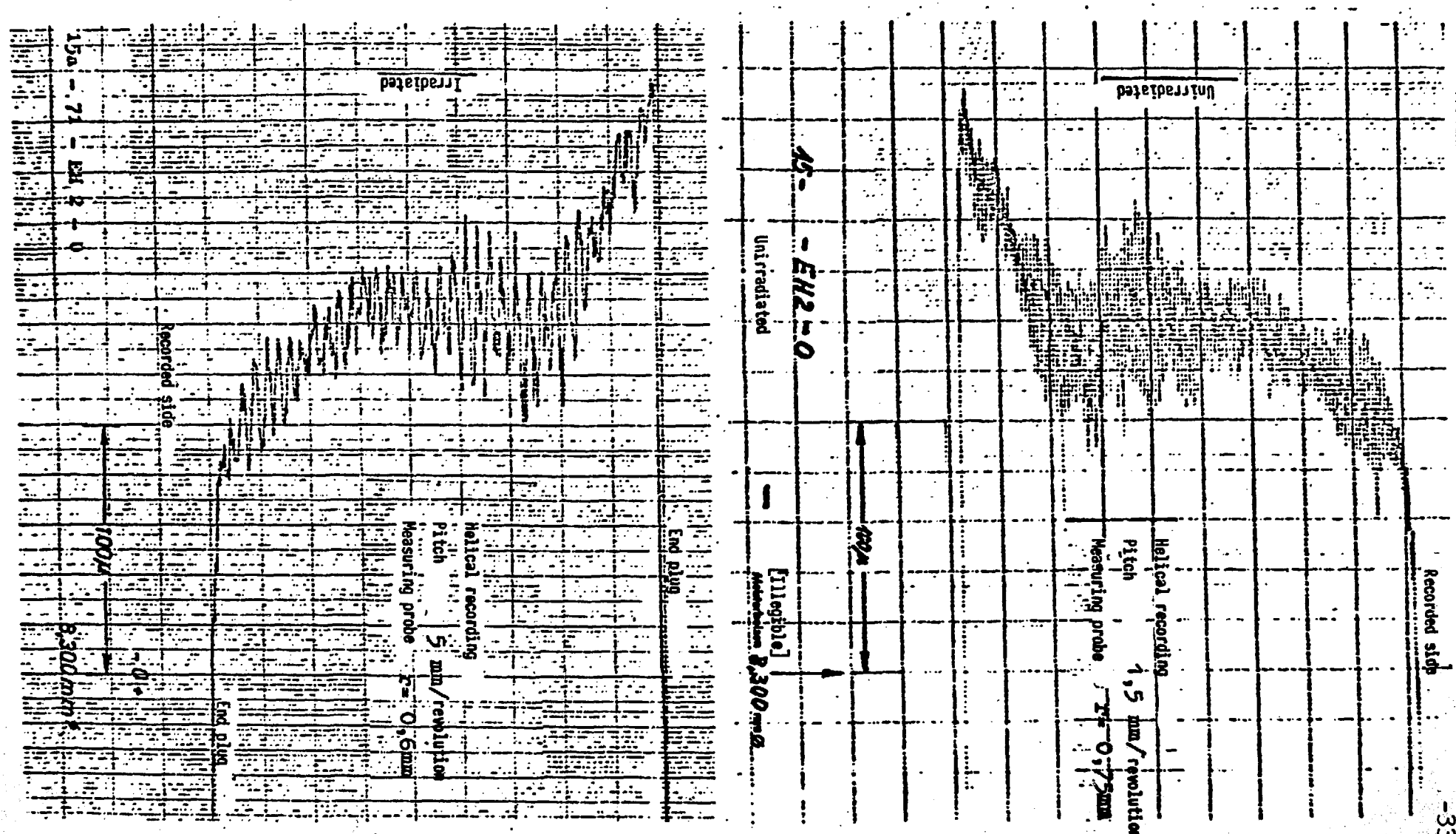

Fig. 18.--Profilometer curves (helical tracing) of a UO_2/Cr specimen before and after irradiation.

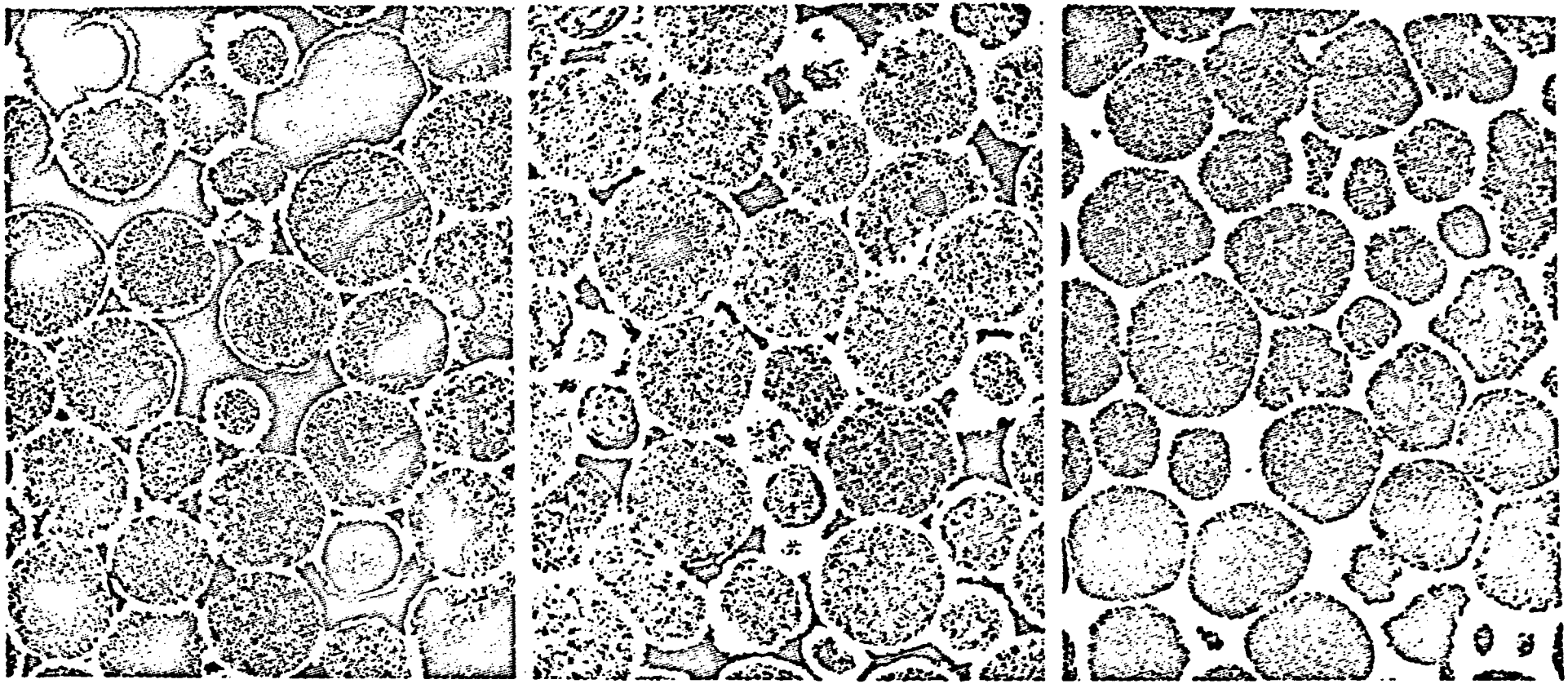

Initial density:

75%TD | 85%TD | 100%TD

Burnup	14 MWd/kg U
Mean rod power	550 W/cm
Mean cladding temp.	650 °C

Fig. 19.--UO_2/Mo cermets of different density after irradiation.

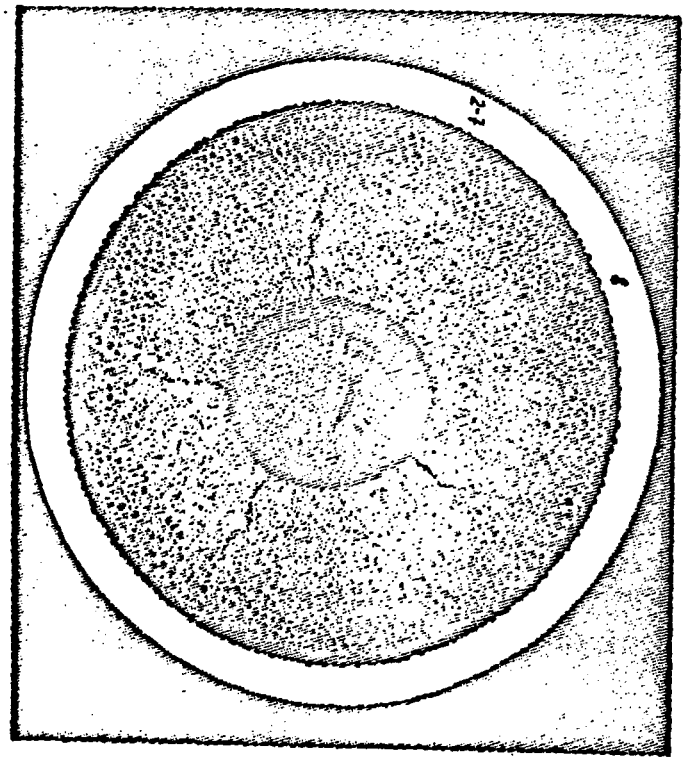

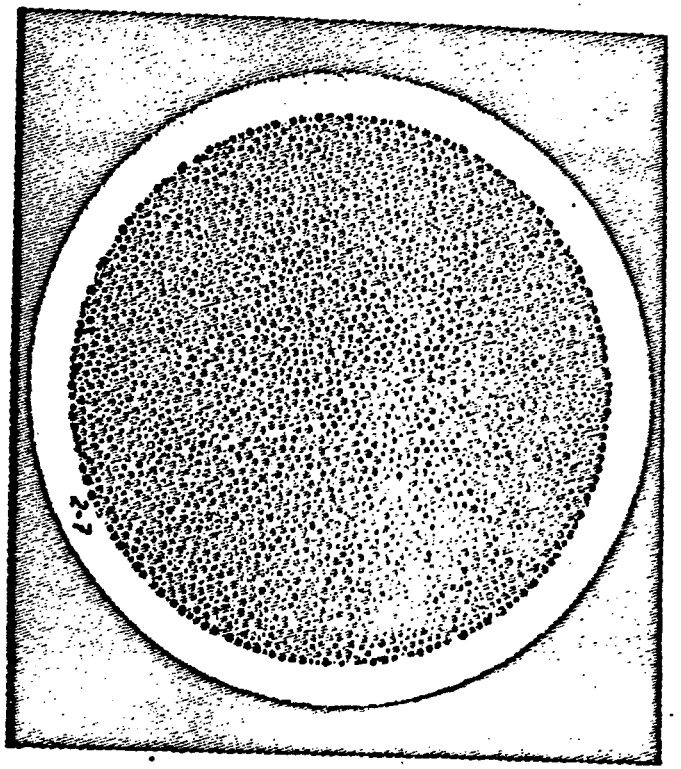

1 mm

20 % Cr

Burnup	84,8 MWd / kg U
Mean rod power	535 W / cm
Mean cladding temp.	600 °C

30 % Cr

Burnup	93,7 MWd / kg U
Mean rod power	510 W / cm
Mean cladding temp.	550 °C

Fig. 20.--UO/Cr cermets after irradiation - transverse microsection.

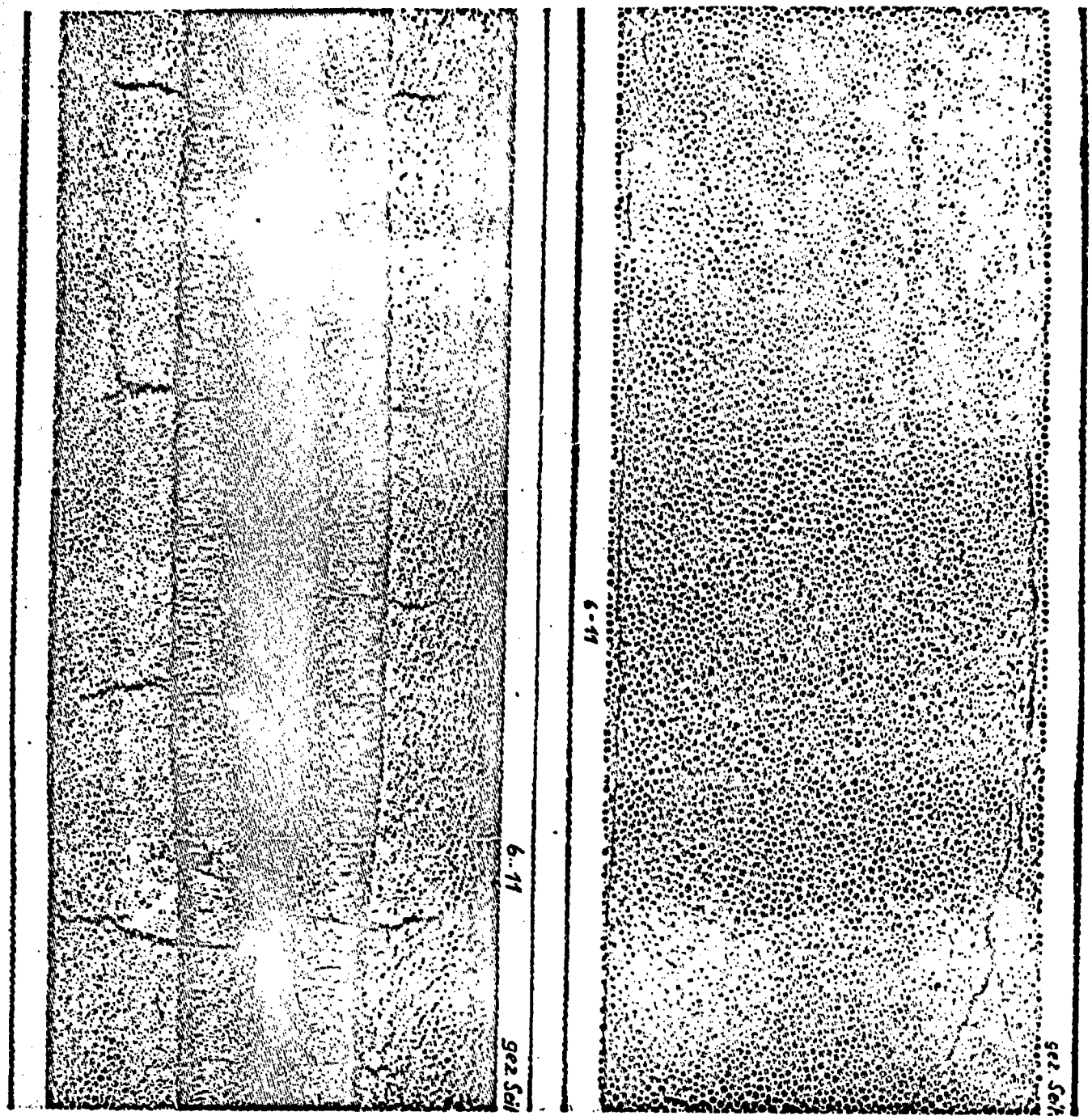

20 % Cr		30 % Cr	
Burnup	95,6 MWd / kg U	Burnup	93,7 MWd / kg U
Mean rod power	600 W / cm	Mean rod power	510 W / cm
Mean cladding temp.	565 °C	Mean cladding temp.	550 °C

Fig. 21.--UO_2/Cr cermets after irradiation - axial microsection.

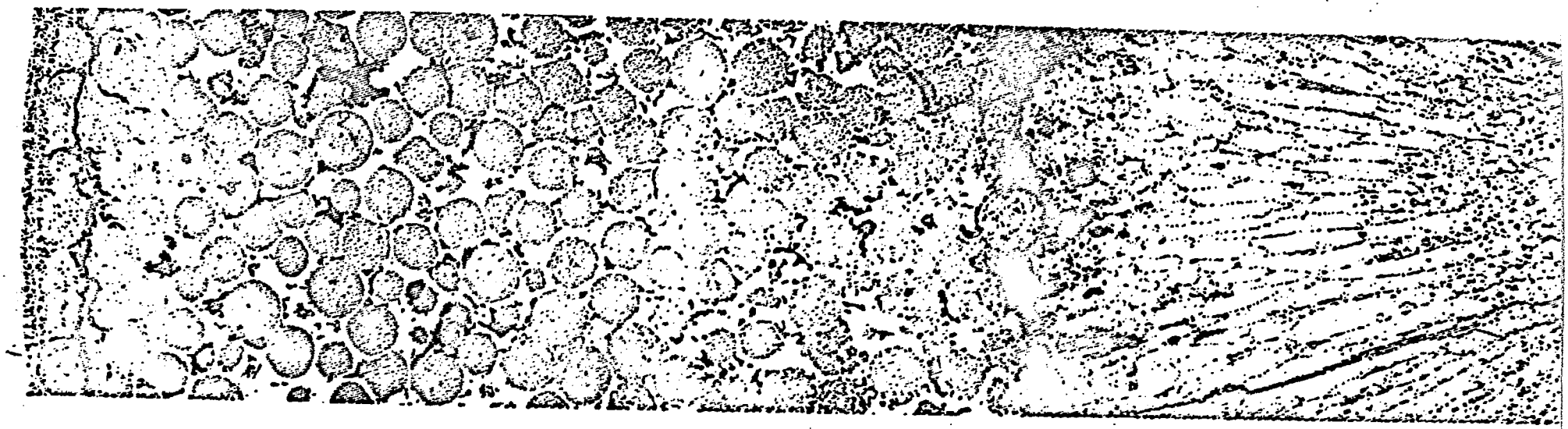

1mm

UO_2 - 20 % Cr, Inconel 625 - cladding

Burnup	60,2 MWd / kg U
Mean rod power	670 W / cm
Mean cladding temp.	550 °C

Fig. 22.--Structure development of specimen D 1 after irradiation as a function of radius.

Outer zone

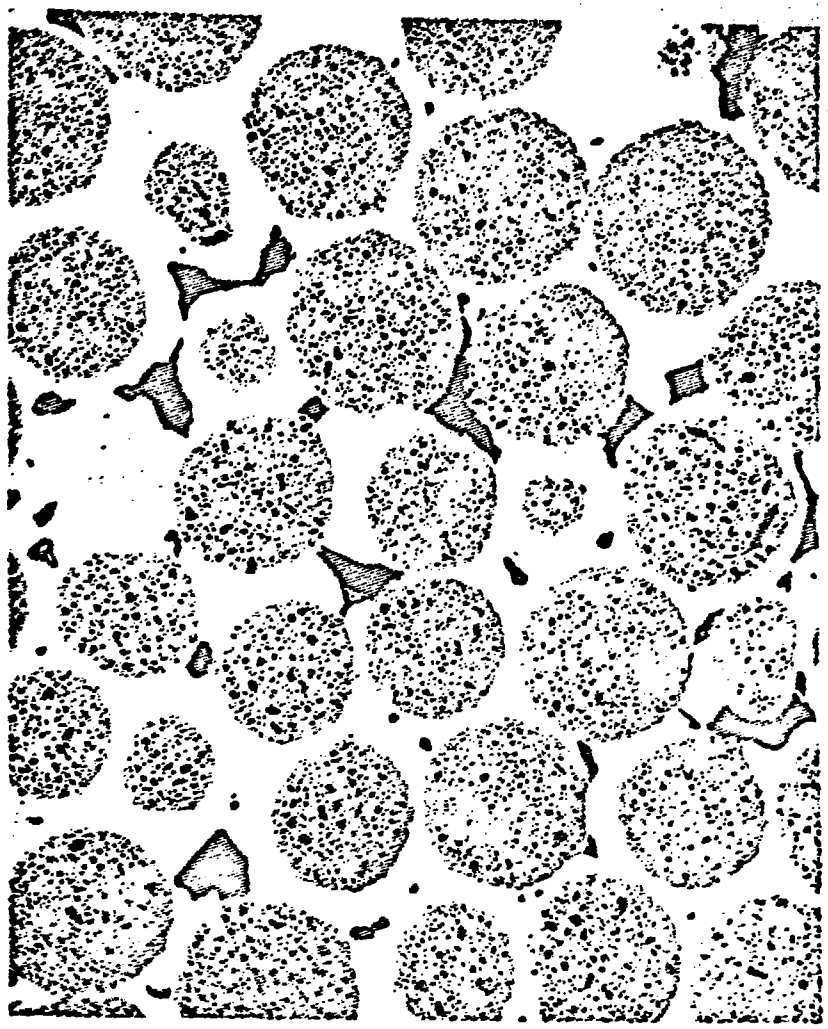

Center

Burnup 93,7 MWd / kg U

Mean rod power 510 W / cm

Mean cladding temp. 550 °C

0,1 mm

Fig. 23.--Structure of specimen E 2 at the outer zone and in the center after irradiation.

Burnup	60,2 MWd/kg U
Mean rod power	560 W/cm
Mean cladding surface temp.	550°C
Maximum cladding surface temp.	690°C

Fig. 24.--Reaction zone between a UO_2/20% Cr cermet and the Inconel 625 cladding.

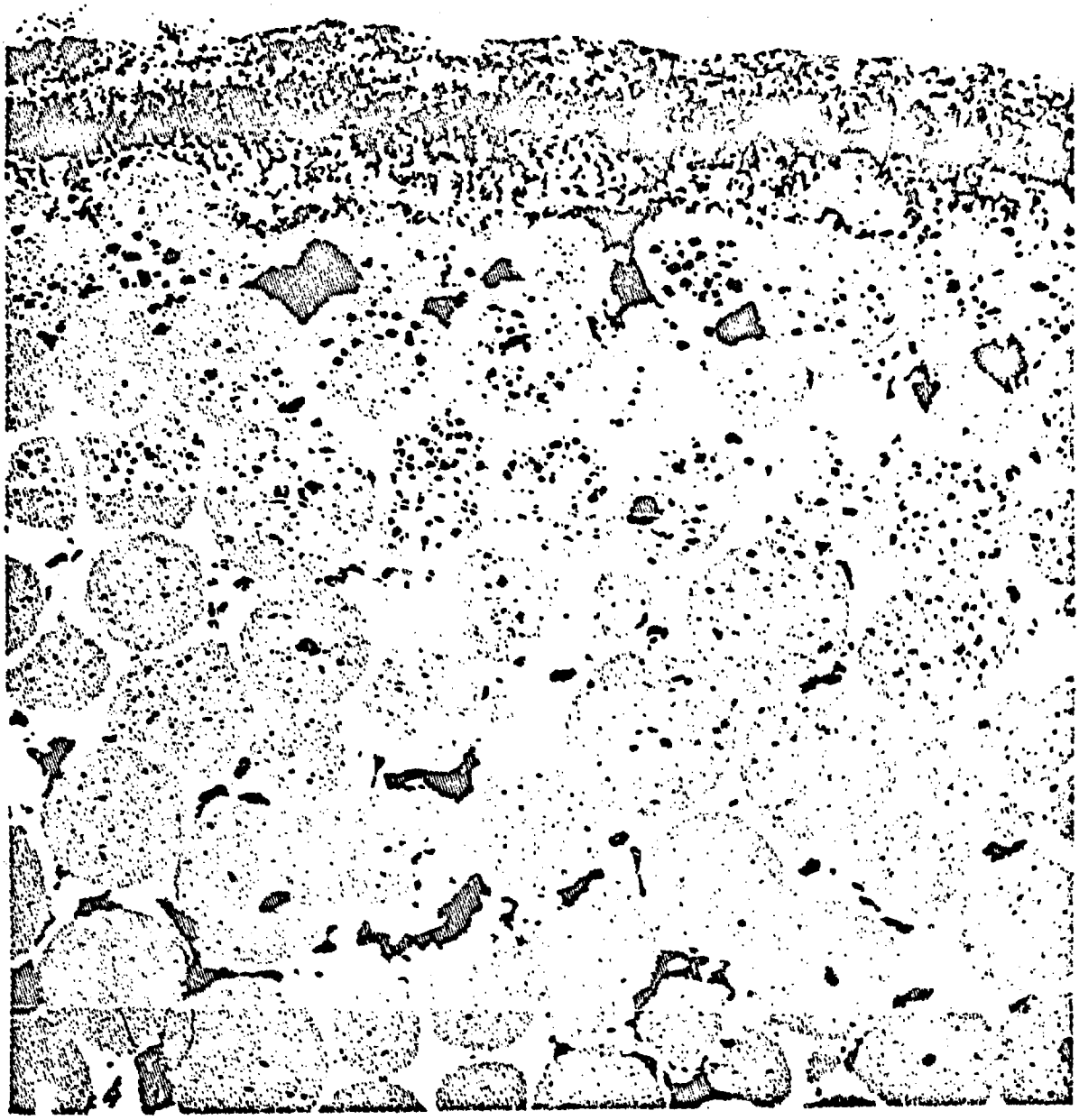

Burnup 58,2 MWd / kg U

Mean rod power 535 W/cm

Mean cladding surface temp. 685 °C

Maximum cladding surface temp. 775 °C

Fig. 25.--Reaction zone between a UO_2/20% Cr cermet and the Hastelloy X cladding.

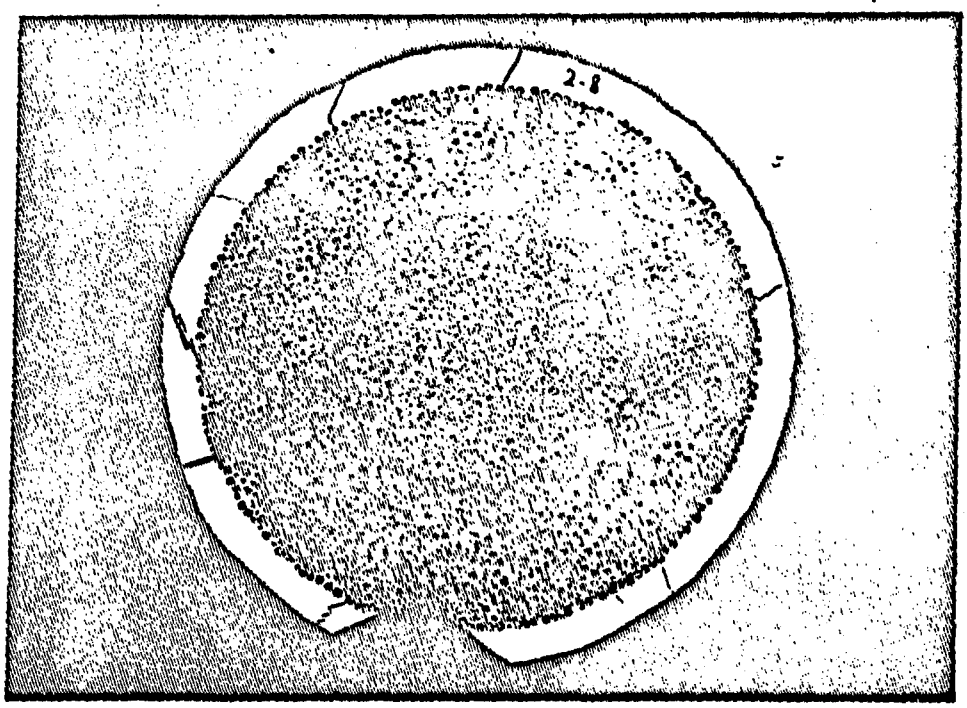

1mm

Burnup	54,4 MWd / kg U
Mean rod power	735 W / cm
Mean cladding surface temp.	690 °C
Maximum cladding surface temp.	750 °C

Fig. 26.--UO_2/20% V cermet with V-cladding after irradiation.

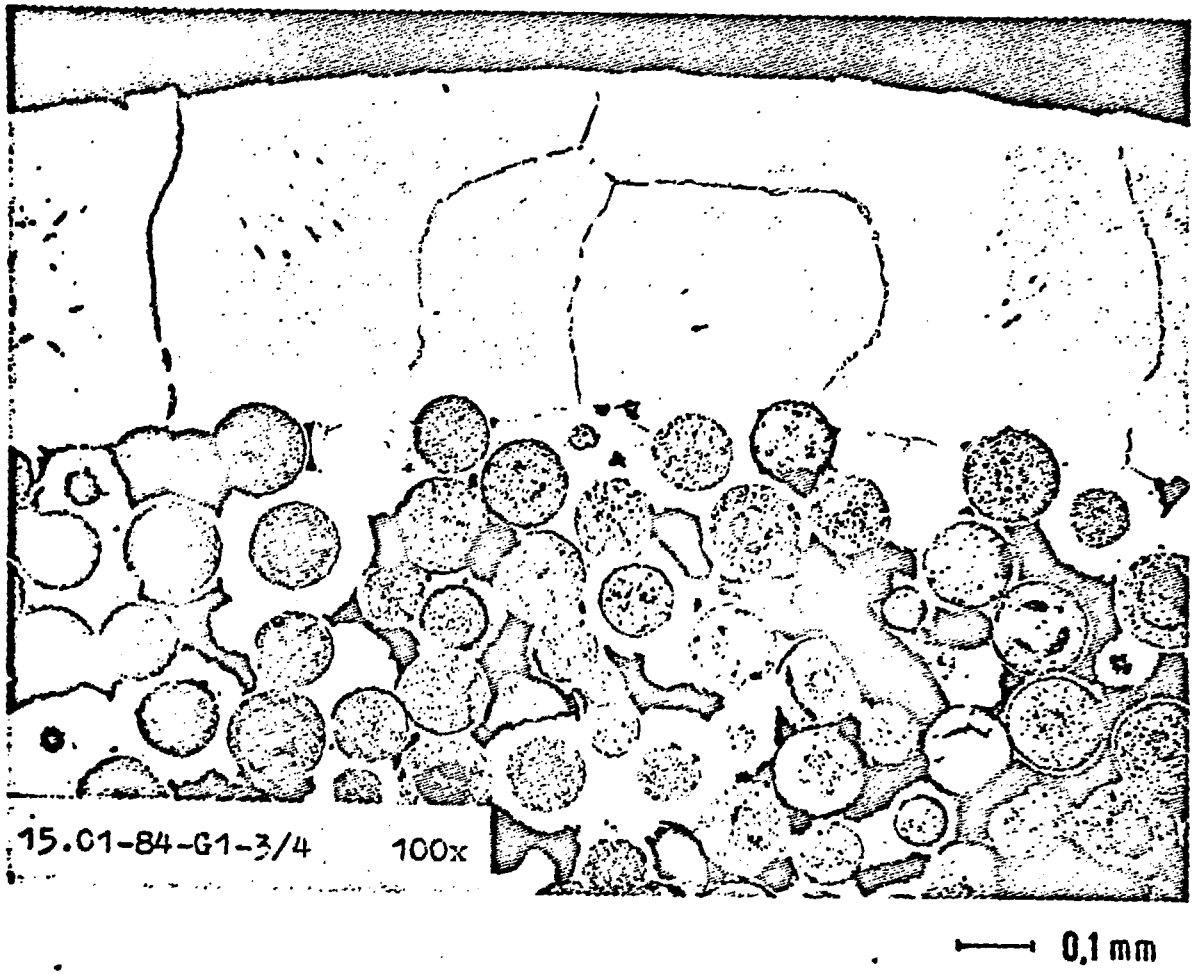

Burnup	17,5 MWd /kg U
Mean rod power	440 W/cm
Mean cladding surface temp	540 °C
Maximum cladding surface temp.	600 °C

Fig. 27.--UO_2/20% V cermet with V-cladding after irradiation--oxide precipitates in the cladding.

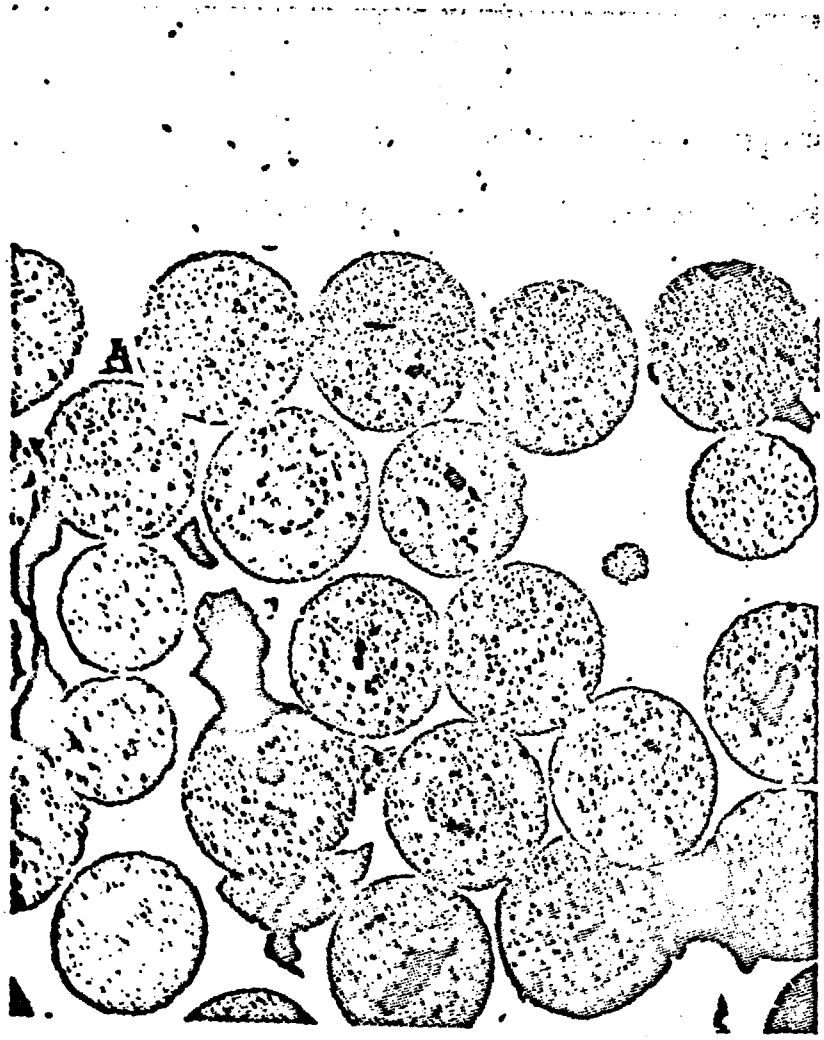

Outer zone

Center

Burnup 54.4 MWd / kg U

Mean rod power 735 W/cm

Mean cladding temperature 690 °C

0.1mm

Fig. 28.--Structure in the outer zone and center of a UO_2/20% V specimen after irradiation.